Alignment-Sensitive Minimax Rates for Spectral Algorithms with Learned Kernels

Dongming Huang, Zhifan Li, Yicheng Li, Qian Lin

Abstract

We study spectral algorithms in the setting where kernels are learned from data. We introduce the effective span dimension (ESD), an alignment-sensitive complexity measure that depends jointly on the signal, spectrum, and noise level σ^2. The ESD is well-defined for arbitrary kernels and signals without requiring eigen-decay conditions or source conditions. We prove that for sequence models whose ESD is at most K, the minimax excess risk scales as $\sigma^2 K$. Furthermore, we analyze over-parameterized gradient flow and prove that it can reduce the ESD. This finding establishes a connection between adaptive feature learning and provable improvements in generalization of spectral algorithms. We demonstrate the generality of the ESD framework by extending it to linear models and RKHS regression, and we support the theory with numerical experiments. This framework provides a novel perspective on generalization beyond traditional fixed-kernel theories.

1 Introduction

Neural networks excel across many applications, yet a complete theoretical understanding of their efficiency remains an open problem. In the infinite-width limit, the Neural Tangent Kernel (NTK) theory approximates training dynamics as kernel regression [23, 2], and it enables the study of generalization by leveraging the classical theory of kernel regression and Reproducing Kernel Hilbert Spaces (RKHS) [8, 48]. However, the NTK theory does not explain why finite-width networks, which adapt their features during training, often outperform traditional methods [19, 16, 25, 37, 43, 36].

A growing line of work directly studies adaptivity, i.e., learning representations or kernel properties during training [4, 27, 31, 10, 47, 50]. Simplified models show that learning *eigenvalues* (with eigenfunctions fixed) can align the kernel with the signal and improve performance [28, 29]. The common thread is signal-kernel alignment: performance improves when the target's energy concentrates on leading eigenfunctions [3, 44, 26, 33]. However, classical RKHS theory relies heavily on fixed spectral assumptions (e.g., polynomial eigenvalue decay) and specific signal regularity conditions (e.g., source conditions) [15], which do not apply to learned spectra. To explain the observed advantages of adaptive kernel methods, we need a refined theoretical framework that goes beyond fixed-kernel assumptions.

In this paper, we propose the **Effective Span Dimension (ESD)**, which is a population complexity measure for the analysis of signal-kernel alignment. ESD counts the smallest number of leading eigenfunctions required so that the remaining signal energy matches the estimation variance. Unlike classical measures that ignore the signal, ESD depends on the *signal, spectrum, and noise level*. Our framework provides new theoretical insights that are absent in classical analyses. In particular, we achieve the following:

1. We establish a sharp minimax optimal convergence rate using ESD.

2. We explain how gradient-based learning algorithms such as the one in Li and Lin [28] adaptively achieve superior generalization by reducing the ESD.

3. We extend our definitions and theory from sequence models to linear regression and kernel regression, which demonstrates the broad applicability of our framework.

Our ESD framework bridges fixed-kernel theory and adaptive learning by quantifying signal-kernel alignment. We hope it will open avenues for deeper understanding of neural networks and novel adaptive algorithms.

Notations. Write $a \lesssim b$ if there exists a constant $C > 0$ such that $a \leq Cb$, and write $a \asymp b$ if $a \lesssim b$ and $b \lesssim a$, where the dependence of the constants on other parameters is determined by the context. For $d \in \mathbb{N}_+$, let $[d] = \{1, 2, \ldots, d\}$; for $d = \infty$, let $[d] = \mathbb{N}_+$. $\mathbf{1}_{\{\cdot\}}$ denotes an indicator function.

2   Background on Kernel Methods

We first review kernel regression to provide context. Let $(\boldsymbol{x}_i, y_i)_{i=1}^n$ be i.i.d. samples from $y = f^*(\boldsymbol{x}) + \epsilon$, where $\boldsymbol{x} \sim \mu$ on a compact space $\mathcal{X}$, ϵ is an independent noise with $\mathbb{E}[\epsilon] = 0, \mathrm{Var}(\epsilon) = \sigma_0^2$. For an estimator $\hat{f}$ of the target function f^*, the excess risk is $\mathcal{R}(\hat{f}; f^*) = \mathbb{E}_{\boldsymbol{x} \sim \mu}\big[(\hat{f}(\boldsymbol{x}) - f^*(\boldsymbol{x}))^2\big]$.

A symmetric, positive-definite, and continuous kernel $\mathbf{k}(\cdot, \cdot) : \mathcal{X} \times \mathcal{X} \to \mathbb{R}$ induces an RKHS $\mathcal{H} \subset L^2(\mathcal{X}, \mu)$ with inner product $\langle \cdot, \cdot \rangle_{\mathcal{H}}$ and norm $\|\cdot\|_{\mathcal{H}}$ [41, 35]. Assuming $\mathbf{k}$ is bounded, Mercer's theorem yields

$$\mathbf{k}\left(\boldsymbol{x}, \boldsymbol{x}'\right) = \sum_{j=1}^{\infty} \lambda_j \psi_j(\boldsymbol{x}) \psi_j\left(\boldsymbol{x}'\right), \quad \boldsymbol{x}, \boldsymbol{x}' \in \mathcal{X}, \tag{1}$$

where $\{\lambda_j\}_{j \geq 1}$ are eigenvalues and $\{\psi_j\}_{j \geq 1} \subset \mathcal{H}$ are eigenfunctions forming an orthonormal basis of $L^2(\mathcal{X}, \mu)$. For background, see Steinwart and Christmann [38], Steinwart and Scovel [39].

Kernel regression estimates f^* using $f = \sum_j \beta_j \psi_j$ and regularizes via a filter of the kernel spectrum $\{\lambda_j\}$[34, 12, 18]. If f^* satisfies the *Hölder source condition* $\sum_j \langle f^*, \psi_j \rangle^2 / \lambda_j^s \leq R_s$ for some positive constants s and R_s [15, 32] and the spectrum decays polynomially $\lambda_j \asymp j^{-\gamma}$, then the minimax rate is $n^{-s\gamma/(s\gamma+1)}$ [48, 30, 42]. The choice of kernels can significantly affect the performance [28, 50], so it is beneficial when the kernel eigenvalues align well with the expansion of the target function.

Since the kernel is usually chosen without knowing f^*, fixed-kernel methods may encounter misalignment. To address this limitation, adaptive methods have recently emerged. For instance, Li and Lin [29] propose adapting kernel eigenvalues while fixing eigenfunctions. Specifically, they consider the kernel $\mathbf{k}_{\boldsymbol{a}}(x, x') = \sum_{j \geq 1} a_j^2 \psi_j(x) \psi_j(x')$ indexed by $\boldsymbol{a} = (a_j)_{j \geq 1}$ and the candidate $f = \sum_{j \geq 1} \beta_j a_j \psi_j$, where a_j's and β_j's are learned jointly via gradient flow. Such adaptation often improves performances, yet classical analyses built on fixed spectral assumptions do not explain these gains, because

1. adapted eigenvalues typically deviate from standard eigenvalue decay assumptions, and

2. it is unclear whether the classical source condition holds with respect to the adapted kernel, and if so, what the value of s is.

We therefore seek a refined theoretical framework that explicitly captures signal-kernel alignment and explain the gains achieved by kernel adaptation.

Bridge to the sequence model. We next connect the RKHS regression with the sequence model to motivate our analysis in the next section. For any $j \in \mathbb{N}_+$, define

$$\theta_j^* = \langle f^*, \psi_j \rangle, \quad z_j = n^{-1} \sum_i y_i \psi_j(\boldsymbol{x}_i), \text{ and } \xi_j = n^{-1} \sum_i \epsilon_i \psi_j(\boldsymbol{x}_i). \tag{2}$$

For large n, we have $n^{-1} \sum_i \psi_j(\boldsymbol{x}_i) \psi_k(\boldsymbol{x}_i) \approx \mathbb{E}[\psi_j(\boldsymbol{x}) \psi_k(\boldsymbol{x})] = \mathbf{1}_{\{j=k\}}$, which implies that

$$z_j \approx \theta_j^* + \xi_j, \text{ and } \mathbb{E}[\xi_j] = 0, \operatorname{Cov}(\xi_j, \xi_k) \approx n^{-1} \sigma_0^2 \mathbf{1}_{\{j=k\}}, \quad \forall j, k \in \mathbb{N}_+. \tag{3}$$

This reduction connects RKHS regression to a sequence model where the observations are $z_j = \theta_j^* + \xi_j$ and the noise terms $\{\xi_j\}$ are uncorrelated with variance $\sigma^2 := n^{-1} \sigma_0^2$. The error in the approximation due to finite n will inflate the estimation variance compared to the sequence model. This approximation error can be controlled if f^* is bounded; see Section 8 for a rigorous treatment.

3 Effective Span Dimension and Span Profile

To bridge existing theory and adaptive kernel methods as discussed in Section 2, we propose a novel framework to characterize the alignment between spectrum and signal. To focus on the main idea, we use the reduction in Equation (3) and first present our framework using sequence models.

Sequence models. A sequence model assumes observations are sampled as follows:

$$z_j = \theta_j^* + \xi_j, \quad 1 \le j \le d, \tag{4}$$

where $d \in \{\infty\} \cup \mathbb{N}_+$, $\boldsymbol{\theta}^* = (\theta_j^*)_{j=1}^d$ is a sequence of unknown parameters, ξ_j's are uncorrelated random variables with mean zero and variance σ^2 (the noise level). For an estimator $\widehat{\boldsymbol{\theta}} = (\widehat{\theta}_j)_{j=1}^d$, we consider the loss $\mathcal{L}(\widehat{\boldsymbol{\theta}}; \boldsymbol{\theta}^*) = \sum_{j=1}^d (\widehat{\theta}_j - \theta_j^*)^2$ and risk $\mathcal{R}(\widehat{\boldsymbol{\theta}}; \boldsymbol{\theta}^*) = \mathbb{E}\mathcal{L}(\widehat{\boldsymbol{\theta}}; \boldsymbol{\theta}^*)$. The sequence model captures core estimation phenomena while permitting explicit analysis [11, 24]. In Section 7, we use whitening to deal with correlated noise and analyze fixed-design linear regression. In Section 8, we leverage the approximation in Equation (3) to analyze RKHS regression and random-design linear regression.

Spectral estimators. Given eigenvalues $\boldsymbol{\lambda} = (\lambda_j)_{j=1}^d$, spectral estimators take the form $\widehat{\theta}_j = (1 - \psi_\nu(\lambda_j)) z_j$, where $\psi_\nu(\lambda)$ is a filter such that larger ν induces more shrinkage. Some examples are:

$$\text{Ridge (R): } \quad \psi_\nu^{\mathrm{R}}(\lambda) = \frac{1}{1 + \lambda/\nu}, \qquad \widehat{\theta}_j^{\mathrm{R},\nu} = \frac{\lambda_j}{\lambda_j + \nu} z_j. \tag{5}$$

$$\text{Gradient Flow (GF): } \quad \psi_\nu^{\mathrm{GF}}(\lambda) = e^{-\lambda/\nu}, \qquad \widehat{\theta}_j^{\mathrm{GF},\nu} = \left(1 - e^{-\lambda_j/\nu}\right) z_j. \tag{6}$$

$$\text{Principal Component (PC): } \quad \psi_\nu^{\mathrm{PC}}(\lambda) = 1_{\{\lambda < \nu\}}, \qquad \widehat{\theta}_j^{\mathrm{PC},\nu} = 1_{\{\lambda_j \ge \nu\}} z_j. \tag{7}$$

For spectral estimators, the risk decomposes into squared bias $\sum_j \left(\psi_\nu(\lambda_j)\right)^2 \theta_j^2$ and variance $\sum_j \left(1 - \psi_\nu(\lambda_j)\right)^2 \sigma^2$, where ν controls the bias-variance trade-off. Classical analyses often assume $\boldsymbol{\theta}^*$ lies in an ellipsoid $\Theta_{\mathbf{a}} = \left\{\theta : \sum_j^\infty a_j^2 \theta_j^2 \leq C^2\right\}$ and derives convergence rates for sequences with $a_i \asymp i^\alpha$[24]. Our theoretical framework aims to bypass these assumptions.

3.1 Effective Span Dimension

Our goal is to develop a measure that captures the interplay between signal structure $\boldsymbol{\theta}^*$, spectrum $\boldsymbol{\lambda}$, and noise variance σ^2. To start, we examine the Principal Component (PC) estimator analytically. PC operates by truncating coordinates with small eigenvalues. Its risk is composed of variance from the retained components and squared bias from those truncated. By trading variance against tail bias, PC admits the optimal truncation point. This motivates our core definition.

Definition 3.1. *Suppose* $\{\lambda_j\}_{j\in[d]}$ *are distinct, with* π_i *indexing the* i-th *largest so that* $\lambda_{\pi_1} > \lambda_{\pi_2} > \ldots$. *We define the Effective Span Dimension (ESD)* $d^\dagger$ *of* $\boldsymbol{\theta}^*$ *w.r.t. the spectrum* $\boldsymbol{\lambda}$ *and variance* σ^2 *as*

$$d^\dagger = d^\dagger(\sigma^2; \boldsymbol{\theta}^*, \boldsymbol{\lambda}) = \min\{k \in [d] : \frac{1}{k} \sum_{i=k+1}^d \left(\theta_{\pi_i}^*\right)^2 \leq \sigma^2\}.$$

Intuitively, the ESD $d^\dagger$ is the number of leading coordinates (with leading eigenvalues λ_i) that are most critical for estimation at a given noise level σ^2. It is the truncation point where the squared tail bias of the PC estimator first becomes comparable to (or less than) the estimation variance. The next theorem shows that $d^\dagger$ describes the best achievable risk for the PC estimator.

Theorem 3.2 (Optimal PC Estimator Risk)**.** *Let* $\widehat{\boldsymbol{\theta}}^{\mathrm{PC},\nu}$ *be the PC estimator for the sequence model in Equation* (4). *Denote by* $\mathcal{R}_*^{\mathrm{PC}}$ *the minimal possible risk over all choices of* ν. *Let* $d^\dagger = d^\dagger(\sigma^2; \boldsymbol{\theta}^*, \boldsymbol{\lambda})$ *be the ESD of* $\boldsymbol{\theta}^*$ *w.r.t. the spectrum* $\boldsymbol{\lambda}$ *and the variance* σ^2. *It holds that*

$$(d^\dagger - 1)\sigma^2 \leq \mathcal{R}_*^{\mathrm{PC}} \leq 2\,d^\dagger \sigma^2.$$

The well-tuned PC estimator is known to be minimax rate optimal under classical assumptions in sequence models that are analogous to the polynomial eigen-decay condition and the source condition in kernel regression (see Propositions 3.11 and 4.23 of Johnstone [24]). In contrast, Theorem 3.2 suggests that we can instead use $O(d^\dagger \sigma^2)$ to upper bound the minimax estimation error with no reliance on particular spectral decay or source conditions. Moreover, the following theorem confirms that $d^\dagger \sigma^2$ indeed characterizes the intrinsic difficulty of estimation.

Theorem 3.3. *For any* $K \in [d]$, *spectrum* $\boldsymbol{\lambda} = \{\lambda_j\}_{j\in[d]}$, *and variance* σ^2, *define*

$$\mathcal{F}_{K,\boldsymbol{\lambda}}^{(n)} = \left\{\boldsymbol{\theta} \in \mathbb{R}^d : d^\dagger(\sigma^2; \boldsymbol{\theta}^*, \boldsymbol{\lambda}) \leq K\right\}. \tag{8}$$

Suppose the sample $\boldsymbol{Z}$ *is drawn from the sequence model in Equation* (4). *We have*

$$\inf_{\widehat{\boldsymbol{\theta}}} \sup_{\boldsymbol{\theta}^* \in \mathcal{F}_{K,\boldsymbol{\lambda}}^{(n)}} \mathcal{R}(\widehat{\boldsymbol{\theta}}, \boldsymbol{\theta}^*) \asymp K\sigma^2,$$

where inf *is taken over any estimator* $\widehat{\boldsymbol{\theta}}$ *based on* $\boldsymbol{Z}$.

Theorem 3.3 considers the minimax risk over $\mathcal{F}_{K,\boldsymbol{\lambda}}^{(n)}$, a class of distributions whose ESDs are at most K. We interpret K as the quota for ESD: the larger K, the larger $\mathcal{F}_{K,\boldsymbol{\lambda}}^{(n)}$ and thus the higher the minimax risk. By Theorem 3.2, it is clear that $2K\sigma^2$ is an upper bound on the minimax risk, and we only need to establish a matched lower bound.

Theorem 3.3 highlights the usefulness of ESD: although we motivate its definition using a specific estimator, it quantifies the best possible (worst-case) performance of *any estimator*. Therefore, the ESD is a fundamental measure for signal-spectrum alignment.

We emphasize that ESD is a population-level complexity measure that depends on the signal and spectrum. It is not a tuning parameter and does not need to be estimated. Its purpose here is explanatory and comparative: it yields a sharp lower bound on the minimax risk and lets us quantify why adaptive learning can outperform fixed-kernel baselines. This mirrors common practice in statistics: sparsity justifies the Lasso, yet practitioners do not estimate the sparsity level before running the method. Estimating ESD from data is an interesting separate problem but orthogonal to our goals in this work.

Comparisons to other alignment measures. Alternative alignment measures exist. The cosine similarity-based kernel-target alignment yields generalization bounds [13, 14], but these bounds are typically too loose to explain fast rates in adaptive kernel methods. Recently, Barzilai and Shamir [7] extended benign-overfitting analyses [6, 40] to kernel ridge regression, which may encounter saturation effects that prevent optimal rates for overly smooth target functions.

Comparisons to other effective dimensions. There are some well-known measures used in the classical analysis of spectral methods. We discuss the differences between ESD and these measures.

Zhang [51] introduces the effective dimension to quantify the complexity of any regularized method. For ridge regularization in Equation (5), the effective dimension is defined as $d_{\text{eff}}(\nu) = \sum_j \frac{\lambda_j}{\lambda_j+\nu}$ (see Proposition A.1 in Zhang [51]). $d_{\text{eff}}(\nu)$ depends only on the spectrum $\boldsymbol{\lambda}$ and the regularization parameter ν, but not on the signal $\boldsymbol{\theta}^*$ or the noise level σ^2. Consequently, the effective dimension is not suitable for measuring signal-spectrum alignment. Furthermore, the effective dimension, as a function of ν, does not directly connect to any minimax risk.

In linear regression, Bartlett et al. [5] analyze the minimum-norm interpolator via the effective rank $r_k = \frac{\sum_{i>k} \lambda_{\pi_i}}{\lambda_{\pi_{k+1}}}$ (using the relationship in Equation (3)). They define the splitting index $k^* = \min\{k \geq 0 : \sigma^2 r_k \geq b\}$ for some constant b and establish risk bounds using $\sigma^2 k^*$. While k^* may resemble ESD since both depend on $\boldsymbol{\lambda}$ and σ^2, they differ in two important aspects: (i) k^* does not involve the signal and thus cannot measure signal-spectrum alignment; and (ii) k^* is tailored to the minimum-norm estimator and does not characterize the minimax risk over a class.

Both $d_{\text{eff}}(\nu)$ and k^* are **signal-agnostic**: they depend on the spectrum $\boldsymbol{\lambda}$ (and either ν or σ^2) only, and therefore remain invariant under any change in the alignment between the signal and the kernel's eigenfunctions. For instance, if adaptive training improves alignment by reordering the eigenfunctions to better align with the signal while preserving the set of

5

eigenvalues, then both $d_{\mathrm{eff}}\left(\nu\right)$ and k^* are unchanged. In contrast, the ESD $d^\dagger\left(\sigma^2;\boldsymbol{\theta}^*,\boldsymbol{\lambda}\right)$ is signal-aware, because it is defined by the bias-variance crossing for the specific $\boldsymbol{\theta}^*$. As signal-kernel alignment improves, the ESD decreases. Consequently, the ESD can mechanistically explain the generalization benefits of adaptive kernel learning, a phenomenon that signal-agnostic complexity measures like $d_{\mathrm{eff}}\left(\nu\right)$ and k^* cannot capture.

Examples. For the following canonical settings, the optimal PC risk satisfies

$$
\mathcal{R}_*^{\mathrm{PC}} \asymp
\begin{cases}
\min\left\{\sigma^{\frac{2s\beta}{1+s\beta}}, d\,\sigma^2\right\}, & (1)\ \lambda_i = i^{-\beta},\ \sum_{i=1}^d \lambda_i^{-s}\theta_i^{*2} \le R,\ \beta, s > 0, \\
\min\left\{\sigma^{2-\frac{2}{\alpha}}, d\,\sigma^2\right\}, & (2)\ \theta_i^* = i^{-\alpha/2},\ \alpha > 1,\ \{\lambda_i\}\downarrow, \\
\min\left\{d\,\sigma^2,\ \log\left(d\sigma^2/\log\left(d\sigma^2\right)\right)\right\}, & (3)\ d < \infty,\ \theta_i^* = i^{-1/2},\ \{\lambda_i\}\downarrow, \\
d\min\left\{d^{-\alpha},\ \sigma^2\right\}, & (4)\ d < \infty,\ 0 < \alpha < 1,\ \theta_i^* = i^{-\alpha/2},\ \{\lambda_i\}\downarrow,
\end{cases}
\tag{9}
$$

where $\{\lambda_i\}\downarrow$ means λ_i is decreasing. Details and proofs are deferred to Section A.3.

In Setting (1), we may take $\sigma^2 = \sigma_0^2/n$ in view of Equation (3), and then the upper bound becomes $\sigma_0^2 \min\left(n^{-\frac{s\beta}{1+s\beta}}, d/n\right)$, which matches the well-known optimal rate under the source condition and the polynomial eigen-decay condition in the case when $d = \infty$. When $d < \infty$, there is a phase transition around $d_0 \asymp n^{\frac{1}{1+s\beta}}$: if $d \lesssim d_0$, the upper bound is $d\sigma_0^2/n$; if $d \gtrsim d_0$, the upper bound is the same as if $d = \infty$.

Section 9.1 illustrates a sparse signal example where the ESD provides a quantitative comparison of two different spectra while the existing measures like $d_{\mathrm{eff}}\left(\nu\right)$ and k^* do not. These examples suggest that the notion of ESD allows us not only to recover classical results but also to explore new settings where the classical framework is inapplicable.

3.2 Span Profile

The definition of ESD explicitly depends on the noise level σ^2, which distinguishes it from other complexity measures in the literature. The dependence on σ^2 reflects the bias-variance trade-off nature of ESD: as σ^2 decreases, more coordinates can be unbiasedly estimated while controlling the overall variance, thereby more bias is removed. To focus on the alignment between a given signal $\boldsymbol{\theta}^*$ and a spectrum $\boldsymbol{\lambda}$, we examine the ESD by varying the noise level.

Definition 3.4. *We define the span profile of $\boldsymbol{\theta}^*$ w.r.t. the spectrum $\boldsymbol{\lambda}$ as $\mathbf{D}_{\boldsymbol{\theta}^*,\boldsymbol{\lambda}} : \tau \mapsto d^\dagger(\tau; \boldsymbol{\theta}^*, \boldsymbol{\lambda})$.*

The span profile $\mathbf{D}_{\boldsymbol{\theta}^*,\boldsymbol{\lambda}}$ is a well-defined object that depends only on $\boldsymbol{\theta}^*$ and the ordering of $\boldsymbol{\lambda}$, and it summarizes how σ^2 affects the ESD. Theorem 3.2 suggests that for two spectra $\boldsymbol{\lambda}^{(1)}$ and $\boldsymbol{\lambda}^{(2)}$, we can compare their alignments with the signal by the ratio of $r(\tau) = \mathbf{D}_{\boldsymbol{\theta}^*,\boldsymbol{\lambda}^{(1)}}(\tau)/\mathbf{D}_{\boldsymbol{\theta}^*,\boldsymbol{\lambda}^{(2)}}(\tau)$ for small τ, because, if this ratio is very small (and in particular if the limit is 0 for $\tau \to 0$), then a kernel method using $\boldsymbol{\lambda}^{(1)}$ can achieve a smaller risk than one that uses $\boldsymbol{\lambda}^{(2)}$. Such comparisons are not as convenient in classical theory. See Section 9 for more illustrations.

A closely related object is the *trade-off function* of $\boldsymbol{\theta}^*$ relative to $\boldsymbol{\lambda}$, which is defined as

$$
\mathbf{H}_{\boldsymbol{\theta}^*,\boldsymbol{\lambda}}(k) \;=\; \frac{1}{k}\sum_{i=k+1}^d \left(\theta_{\pi_i}^*\right)^2 \;=\; \frac{1}{k}\sum_{i:\,\lambda_i < \lambda_{\pi_k}} \left(\theta_i^*\right)^2, k \in [d].
\tag{10}
$$

The quantity $\sigma^{-2}\mathbf{H}_{\boldsymbol{\theta}^*,\boldsymbol{\lambda}}(k)$ equals the bias-variance ratio of the PC estimator using the k leading coordinates. Properties of span profiles and trade-off functions are summarized as follows.

Proposition 3.5. *(1) Both* $\mathbf{D}_{\boldsymbol{\theta}^*,\boldsymbol{\lambda}} : \tau \mapsto [d]$ *and* $\mathbf{H}_{\boldsymbol{\theta}^*,\boldsymbol{\lambda}} : [d] \mapsto [0,\infty)$ *are nonincreasing. (2) For any* τ, *it holds that* $\mathbf{D}_{\boldsymbol{\theta}^*,\boldsymbol{\lambda}}(\tau) = \min\{k \in [d] : \quad \mathbf{H}_{\boldsymbol{\theta}^*,\boldsymbol{\lambda}}(k) \leq \tau\}$. *(3) For two spectra* $\boldsymbol{\lambda}^{(1)}$ *and* $\boldsymbol{\lambda}^{(2)}$, *if* $\mathbf{H}_{\boldsymbol{\theta}^*,\boldsymbol{\lambda}^{(1)}}(k) \leq \mathbf{H}_{\boldsymbol{\theta}^*,\boldsymbol{\lambda}^{(2)}}(k)$ *for all* $k \in [d]$, *then* $\mathbf{D}_{\boldsymbol{\theta}^*,\boldsymbol{\lambda}^{(1)}}(\tau) \leq \mathbf{D}_{\boldsymbol{\theta}^*,\boldsymbol{\lambda}^{(2)}}(\tau), \quad \forall \tau > 0$.

Property (3) in Theorem 3.5 suggests that the faster $\mathbf{H}_{\boldsymbol{\theta}^*,\boldsymbol{\lambda}}(\cdot)$ decreases, the better the spectrum $\boldsymbol{\lambda}$ aligns with the signal $\boldsymbol{\theta}^*$. In the extreme case where the ordering of λ_i matches the ordering of $|\theta_i^*|^2$, the decay of $\mathbf{H}_{\boldsymbol{\theta}^*,\boldsymbol{\lambda}}(\cdot)$ is the fastest, which leads to the most favorable span profile.

4 Minimax Optimal Convergence Rates

When using the span profile to characterize the signal-spectrum alignment, it is of interest to establish the optimal convergence rates. Since the setting where $d = d_n$ grows along with n has been studied in Theorem 3.3, we focus on the case where $d = \infty$ and the spectrum $\boldsymbol{\lambda}$ is given with ordering denoted by $\{\pi_j\}$ such that $\lambda_{\pi_1} > \lambda_{\pi_2} > \ldots$. For the convenience of the asymptotic analysis, we examine the span profile at $\tau = \sigma_0^2/n$, where σ_0^2 is fixed and n enumerates $\mathbb{N}_+$.

We begin by defining a class of populations whose span profile is bounded by a sequence of quotas $\boldsymbol{K} = \{K_n\}_{n=1}^\infty$. This leads to the following class of parameters:

$$\mathcal{F}_{\boldsymbol{K},\boldsymbol{\lambda}} := \left\{ \boldsymbol{\theta} \in \mathbb{R}^\infty : \mathbf{D}_{\boldsymbol{\theta},\boldsymbol{\lambda}}\left(\frac{\sigma_0^2}{n}\right) \leq K_n, \quad \forall\, n \geq n_0 \text{ for some } n_0 \right\}. \tag{11}$$

For each $\boldsymbol{\theta} \in \mathcal{F}_{\boldsymbol{K},\boldsymbol{\lambda}}$, the sequence model in Equation (4) with $\boldsymbol{\theta}^* = \boldsymbol{\theta}$ and $\sigma^2 = \sigma_0^2/n$ will have an ESD no greater than K_n. For a sample $\boldsymbol{Z}^{(n)}$ from this sequence model and any estimator $\widehat{\boldsymbol{\theta}}$ based on $\boldsymbol{Z}^{(n)}$, we aim to determine the convergence rate of the following minimax risk:

$$\inf_{\widehat{\boldsymbol{\theta}}} \sup_{\boldsymbol{\theta} \in \mathcal{F}_{\boldsymbol{K},\boldsymbol{\lambda}}} \mathcal{R}(\widehat{\boldsymbol{\theta}}, \boldsymbol{\theta}). \tag{12}$$

We emphasize that $\boldsymbol{K}$ is a *model-class descriptor*. It is not a parameter of the distribution, but rather describes a condition on the distribution. For example, the sparsity assumption in high-dimensional regression states that $\|\boldsymbol{\beta}\|_0 \leq s$, so s describes a class of distributions; yet s is not a parameter of the distribution. Our minimax result requires a regularity condition on the quota sequence $\boldsymbol{K}$. Let $\bar{K} := \sup\{K_n\} \in \mathbb{N} \cup \{\infty\}$. For any $k \in [\bar{K}]$, let $M_k := \max\{n : K_n = k\}$ (the largest n such that $K_n = k$).

Condition 4.1. *(1)* $K_{n+1} - K_n \leq 1$ *for all* n *sufficiently large. (2) For all* $k \in [\bar{K}]$, *it holds that* $(k+1)/M_{k+1} \leq k/M_k$.

Theorem 4.1 ensures that K_n does not grow faster than n, and the ratio sequence $\{k/M_k\}$ is nonincreasing. Theorem 4.1 is easily satisfied by common growth laws.

Example 4.2. *(1) Suppose* $K_n \asymp n^a$ *where* $0 < a < 1$. *For any* k, *we have* $L_k \asymp M_k \asymp k^{1/a}$. *Since* $k/k^{1/a}$ *is decreasing, Theorem 4.1 holds.*
(2) Suppose $K_n \asymp (\log n)^b$ *where* $b > 0$. *For any* k, *we have* $L_k \asymp M_k \asymp e^{k^{1/b}}$. *Since* $k/e^{k^{1/b}}$ *is decreasing, Theorem 4.1 holds.*

The next theorem provides a lower bound on the minimax risk in Equation (12).

Theorem 4.3. *Suppose Theorem 4.1 holds for a quota sequence $\boldsymbol{K} = \{K_n\}_{n=1}^{\infty}$. Let $c_0 = 1/4$. If $\boldsymbol{Z}^{(n)}$ is drawn from the sequence model with $\boldsymbol{\theta}^* = \boldsymbol{\theta}$ and $\sigma^2 = \sigma_0^2/n$, it holds that*

$$\inf_{\widehat{\boldsymbol{\theta}}} \sup_{\boldsymbol{\theta} \in \mathcal{F}_{\boldsymbol{K},\boldsymbol{\lambda}}} \mathcal{R}(\widehat{\boldsymbol{\theta}}, \boldsymbol{\theta}) \geq c_0 \sigma_0^2 \frac{K_n}{n}.$$

Theorem 4.3 shows that given a quota sequence $\boldsymbol{K}$, no estimator can, uniformly over the class $\mathcal{F}_{\boldsymbol{K},\boldsymbol{\lambda}}$, achieve a faster convergence rate of risk than $\sigma_0^2 K_n/n$. On the other hand, Theorem 3.2 (using $\sigma^2 = \sigma_0^2/n$) provides a matched upper bound on the risk of the optimal PC estimator, which is $2\sigma_0^2 K_n/n$. We thus conclude that the minimax optimal rate over $\mathcal{F}_{\boldsymbol{K},\boldsymbol{\lambda}}$ is $\sigma_0^2 K_n/n$.

Since our theory does not invoke any source condition or eigenvalue-decay condition, it goes beyond the classical analysis in the literature. It suggests that the ESD is an essential quantity, and the span profile provides a useful characterization of the attainable error rate for spectral methods.

To see why our framework is more general, the next example presents a case where the minimax convergence rate is slower than the rate in the fixed-dimensional setting while being faster than the standard rate in classical infinite-dimensional settings.

Example 4.4. *Let $b \geq 1$ be a constant and $K_n = \lceil (\log n)^{1/b} \rceil$ for $n \in \mathbb{N}_+$. Suppose $\{\lambda_j\}_{j=1}^{\infty}$ is decreasing and $\theta_{j+1}^* = \sqrt{\sigma_0^2 \left[je^{-j^b} - (j+1)e^{-(j+1)^b} \right]}$ for $j \geq 1$ and $\theta_1^* = 0$. Then, $\boldsymbol{\theta}^* \in \mathcal{F}_{\boldsymbol{K},\boldsymbol{\lambda}}$ and the optimal rate is $\sigma_0^2 (\log n)^{1/b} n^{-1}$. In contrast, the traditional convergence rate based on the source condition is $\sigma_0^2 n^{-\alpha/(1+\alpha)}$ for arbitrary $\alpha > 0$, which is not sharp.*

5 Adaptive eigenvalues via over-parameterized gradient flow

This section will investigate the benefits of learning eigenvalues via over-parameterized gradient flow (OP-GF) in sequence models [28] through the lens of ESDs. Section 9.2 outlines the framework to explain the benefits of adaptive kernels and presents an experiment using a linear network. Analyzing eigenfunction evolution theoretically is more difficult and is left for future work.

Inspired by the over-parameterized nature of deep neural networks, Li and Lin [28] parameterized $\theta_j = a_j b_{j,1} \cdots b_{j,D} \beta_j$, where D stands for the number of layers and $(a_j, b_{j,i}, \beta_j)$ are parameters to be learned. The gradient flow w.r.t. the empirical loss $L = \frac{1}{2} \sum_j (\theta_j - y_j)^2$ is given by

$$\dot{a}_j = -\nabla_{a_j} L, \quad \dot{b}_{j,i} = -\nabla_{b_{j,i}} L \quad (i \in [D]), \quad \dot{\beta}_j = -\nabla_{\beta_j} L, \tag{13}$$
$$a_j(0) = \lambda_j^{1/2}, \quad b_{j,i}(0) = b_0 > 0, \quad (i \in [D]), \quad \beta_j(0) = 0, \quad j \in [d],$$

where λ_j's are the initial eigenvalues and b_0 is the common initialization of all $b_{j,i}$. At time t, the learned eigenvalues are given by $\tilde{\lambda}_j(t) = (a_j(t)b_{j,1}(t) \cdots b_{j,D}(t))^2$ and the OP-GF estimates are $\hat{\theta}_j^{OP}(t) = \tilde{\lambda}_j^{\frac{1}{2}}(t)\beta_j(t)$ for $j \in [d]$. Li and Lin [28] consider infinite-dimensional sequence models with a polynomial decay condition on the initial eigenvalues and establish upper bounds on the risk of the OP-GF estimator with proper early stopping.

Here we study the dynamics of eigenvalues in OP-GF and how it changes the ESD. At time t, the learned eigenvalues are $\tilde{\boldsymbol{\lambda}}(t) := (\tilde{\lambda}_j(t))_{j \in [d]}$, and the ESD is $d^\dagger(t) = d^\dagger(\sigma^2; \boldsymbol{\theta}^*, \tilde{\boldsymbol{\lambda}}(t))$. We aim to show that under some regularity conditions, OP-GF can adjust the ordering of eigenvalues $\tilde{\boldsymbol{\lambda}}(t)$ to reduce the ESD $d^\dagger(t)$, which leads to a better signal-spectrum alignment.

We begin with some notations for the sequence model in Equation (4). We focus on the *large-sample case* where $\sigma^2 = \frac{\sigma_0^2}{n}$ and $\sigma_0 = 1$ without loss of generality. Denote $\tilde{d} = \sum_{i=1}^d \lambda_i$ (i.e., sum of initial eigenvalues). Let $\pi_t^{-1}(i)$ denote the rank of $\tilde{\lambda}_i(t)$ at time t.

Assumption 5.1. *We assume (1) Each noise ξ_j in Equation (4) is sub-Gaussian with variance proxy bounded by $C_{proxy}\sigma^2$.   (2) Let $\varepsilon = 2C_{proxy}^{-1/2} n^{-1/2} \sqrt{\ln n \tilde{d} \cdot \ln n}$ and $\varepsilon' = 2C_{proxy}^{-1/2} n^{-1/2} \sqrt{\ln n}$. Define $S := \{j \in [d] : |\theta_j^*| > \varepsilon\}$. We have $|S| \leq n$.   (3) $\inf_{j \in S} \lambda_j > n^{-\delta}$ for some $\delta \in (0, 1)$.*

Theorem 5.2. *Suppose that Theorem 5.1 holds and the initialization in Equation (13) is $b_0 = c_B D^{\frac{D+1}{D+2}} \varepsilon^{\frac{1}{D+2}}$. Define $t_2 = C \cdot D^{\frac{D}{D+2}} (\varepsilon)^{-\frac{2D+2}{D+2}}$. There exist some constants c, C, C_M, C_{max}, C_η, c_η, c_B, and c', such that with probability larger than $1 - 4/n$, we have*

$$d^\dagger(t_2) \leq d^\dagger(t_1)$$

for any $t_1 \in [0, t_2)$ if the followings hold:

1. *For any $j \in S$, we have $M \leq |\theta_j^*|$, where $M := C_M \varepsilon$;*

2. *For any $j \in S^c$, we have $|\theta_j^*| \leq \tilde{\sigma}$, where $\tilde{\sigma} = c'\varepsilon$.*

3. *For any $i, j \in S$, let $\eta_{i,j} := |\theta_i^*| - |\theta_j^*|$. At least one of the followings hold: (a) $\eta_{i,j} \leq 0$, (b) $\eta_{i,j} \geq C_\eta \varepsilon$ and $|\theta_i^*| \leq C_{max} M$, or (c) $\frac{|\theta_i^*|}{|\theta_j^*|} > (1 + \frac{c_\eta}{D})$.*

4. *At time t_1, define two subsets of S^c: $A_1 := \{i \in S^c : \pi_{t_1}^{-1}(i) < d^\dagger(t_1), \lambda_i < c \cdot D^{-\frac{D}{D+2}} \cdot M^{\frac{2}{D+2}}\}$ and $B_1 := \{i \in S^c : \pi_{t_1}^{-1}(i) > d^\dagger(t_1)\}$, and define a subset of S: $B_2 := \{i \in S : \pi_{t_1}^{-1}(i) > d^\dagger(t_1)\}$. It holds that $|B_2| + \min[(|A_1| - |B_2|)_+, |B_1|] \leq |B_2|(C_M/c')^2$.*

Theorem 5.2 shows that OP-GF reduces the ESD. The conditions ensure that strong signals with small initial eigenvalues have larger adapted eigenvalues than weak signals.

6   Numerical experiments

Data Generation. We utilize the **misalignment** setting in Li and Lin [28] to specify a d-dimensional sequence model. We fixed the eigen-decay rate $\gamma > 0$, the signal decay rate $p > 0$, and the number of nonzero signals J. Given any misalignment parameter $q \geq 1$, we set eigenvalues as $\lambda_j = j^{-\gamma}, j \in [d]$, and set the true nonzero parameters as $\theta_{\ell(j)}^* = C \cdot j^{-\frac{p+1}{2}}$, where $\ell(j) = [j^q]$ and $j \leq J$. Here all other elements of θ_j^* are zero and $d \geq J^q$ so $\|\boldsymbol{\theta}^*\|_0 = J$. The observations are sampled as $y_i \sim N(\theta_i^*, \sigma^2)$. This setting provides a flexible way to control the alignment between the signal structure and the spectrum. When $q = 1$, the ordering of $\boldsymbol{\theta}^*$ align perfectly with the ordering of $\boldsymbol{\lambda}$. As q increases, more nonzero elements of $\boldsymbol{\theta}^*$ are located on the tail where the eigenvalues are smaller, and more large eigenvalues are associated with zero signals, creating a worse signal-spectrum alignment.
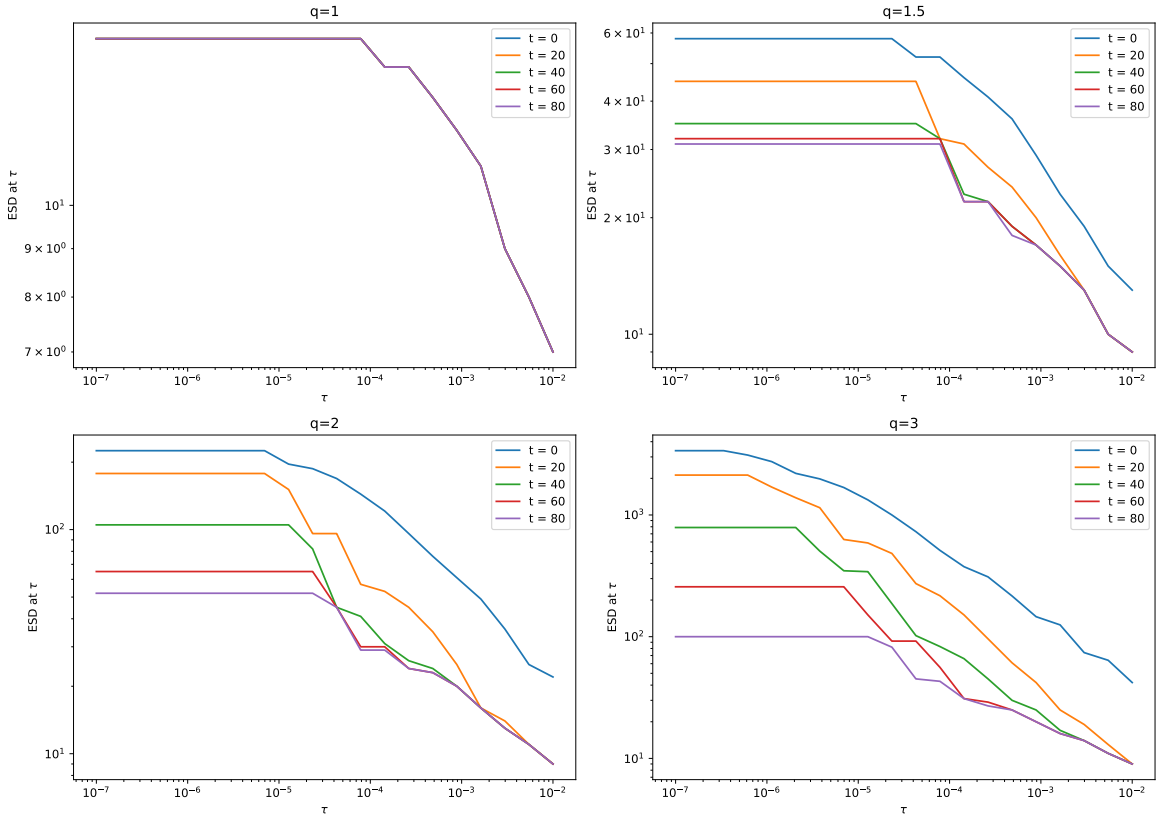
Figure 1: Evolution of span profiles during the training of an over-parameterized gradient flow. The misalignment level q varies from 1 to 3. Fixed parameters are $n = 10000$, $\sigma_0 = 1$, $d = 5000$, $J = 15$, $p = 2.5$, and $\gamma = 1$.

Evolution of Span Profile The first experiment visualizes the span profile of the signal w.r.t. the learned spectrum at various stages in the OP-GF process with $D = 0$. Given a sample, we approximate the gradient flow in Equation (13) by discrete-time gradient descent and obtain the solution $\{(a_j(t), \beta_j(t))_{t \geq 0} : j \in [d]\}$. The trained eigenvalue sequence $\tilde{\boldsymbol{\lambda}}(t)$ at time t is given by $\tilde{\lambda}_j(t) = a_j^2(t)$ for $j \in [d]$. Here we focus on time points before the optimal stopping time. Figure 1 illustrates the evolution of the span profile w.r.t. the learned spectrum for different training times t and various values of q.

When $q = 1$ (Top-Left panel), the span profiles at different training times t are nearly identical. This is because the initial spectrum already aligns perfectly with the signal and there is no room for improvement. For $q > 1$ (Top-Right, Bottom-Left, Bottom-Right panels), we observe that as the training time t increases 0 to 80, the span profile shifts downwards. This suggests that the training process refines the alignment between the spectrum and the signal. In addition, the reduction in the span profile is more significant for $q = 3$ compared to $q = 1.5$, because $q = 3$ corresponds to a greater initial misalignment between the signal and the spectrum, rendering the improvement from OP-GF more substantial.

Evolution of ESD and Estimation Error of PC Estimators We next empirically investigate the evolution of the ESD $d^\dagger$ and the estimation error as well as the impact of layers D. At any time t, we compute the ESD $d^\dagger(t)$ based on the learned eigenvalue sequence $\tilde{\boldsymbol{\lambda}}(t)$ $\tilde{\boldsymbol{\lambda}}(t)$ and also the PC estimate $\widehat{\boldsymbol{\theta}}(t)$ based on $\tilde{\boldsymbol{\lambda}}(t)$, with number of components determined by $d^\dagger(t)$. Theorems 3.2 and 3.3 suggest that the PC estimator tuned by the ESD can achieve the minimax risk rate, so we expect $\widehat{\boldsymbol{\theta}}(t)$ to perform well.
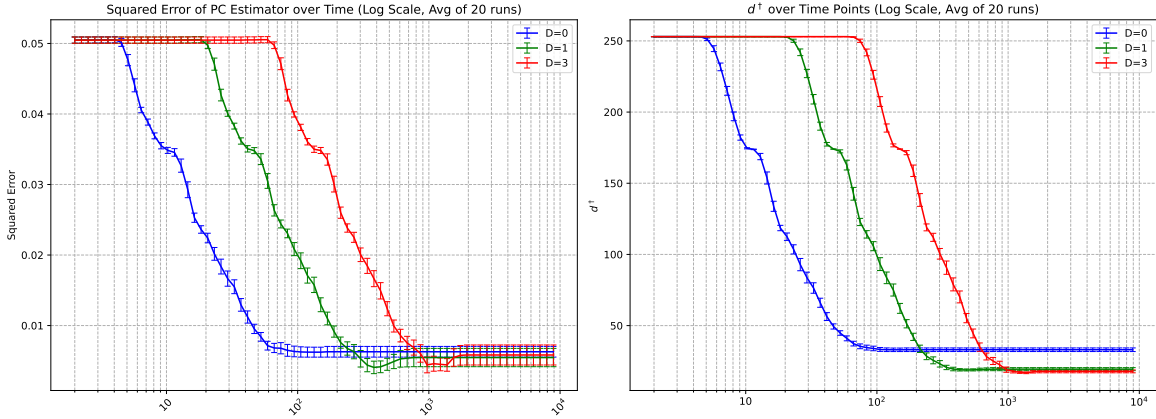

Figure 2: Averaged squared error of the tuned PC estimator and ESD as a function of the training time. Each average is computed based on 20 replications and each error bar represents a standard deviation.

The empirical evaluation involved 20 Monte Carlo repetitions. Figure 2 displays the averaged $d^\dagger(t)$ and the averaged estimation error of $\widehat{\boldsymbol{\theta}}(t)$ in Figure 2 as a function of training time t. We observe that both the ESD and the squared error of the tune PC estimator exhibit a general decay trend over training time t. Furthermore, for the shallow model with $D = 0$ (with no $b_{i,j}$ parameters), the initial decrease in ESD and MSE occurs earlier compared to the deeper models with $D = 1$ or $D = 3$. However, with sufficient training iterations, the

11

deeper models with $D = 1$ or $D = 3$ can achieve lower ESD values than the shallow model with $D = 0$. These findings suggest that increased model depth ($D > 0$) may facilitate a better adaptation of the spectrum, and thus lead to lower estimation error. This observation offers a perspective on the benefits of depth in spectral learning, but a comprehensive study for general models is left for future research.

7 Extension to Correlated Noise and Fixed-design Linear Model

This section extends the concepts of ESD and span profile, developed in Section 3 for the sequence model, to the setting of fixed design linear regression. In addition, we demonstrate how the minimax optimal prediction risk in this setting can be characterized using the span profile, paralleling the analysis in Section 4.

7.1 Strategy of reduction

Before introducing the linear model, it is helpful to outline our general transformation strategy in the context of a sequence model with correlated noise. Suppose $d \in \mathbb{N}_+$ and the observations is

$$\mathbf{Z} = \boldsymbol{\theta}^\star + \boldsymbol{\xi}, \quad \boldsymbol{\xi} \sim \mathcal{N}_d \left(0, \sigma^2 \boldsymbol{\Sigma}_\xi \right) \tag{14}$$

where $\boldsymbol{\Sigma}_\xi \in \mathbb{R}^{d \times d}$ is known, symmetric, and positive definite. For correlated sequence model, it is usually of interest to measure the estimation error using the squared Mahalanobis distance defined as $L(\boldsymbol{\theta}^\star, \widehat{\boldsymbol{\theta}}^\star) = (\widehat{\boldsymbol{\theta}}^\star - \boldsymbol{\theta}^\star)^\top \boldsymbol{\Sigma}_\xi^{-1} (\widehat{\boldsymbol{\theta}}^\star - \boldsymbol{\theta}^\star)$.

Let $\mathbf{L} = \boldsymbol{\Sigma}_\xi^{-1/2}$ be a symmetric square root of $\boldsymbol{\Sigma}_\xi^{-1}$. Define the whitened observation and transformed parameters as

$$\tilde{\mathbf{Z}} = \mathbf{L}\mathbf{Z}, \quad \tilde{\boldsymbol{\theta}}^\star = \mathbf{L}\boldsymbol{\theta}^\star.$$

It follows that $\tilde{\mathbf{Z}} = \tilde{\boldsymbol{\theta}}^\star + \tilde{\boldsymbol{\xi}}$, where $\tilde{\boldsymbol{\xi}} = \mathbf{L}\boldsymbol{\xi} \sim \mathcal{N}_d \left(0, \sigma^2 \mathbf{I}_d \right)$. Accordingly, any estimator $\widehat{\boldsymbol{\theta}}$ for $\boldsymbol{\theta}^\star$ is equivalent to the estimator $\widehat{\tilde{\boldsymbol{\theta}}} := \mathbf{L}\widehat{\boldsymbol{\theta}}$ for $\tilde{\boldsymbol{\theta}}^\star$, whose squared loss is $\|\widehat{\tilde{\boldsymbol{\theta}}} - \tilde{\boldsymbol{\theta}}^\star\|^2 = (\widehat{\boldsymbol{\theta}}^\star - \boldsymbol{\theta}^\star)^\top \boldsymbol{\Sigma}_\xi^{-1} (\widehat{\boldsymbol{\theta}}^\star - \boldsymbol{\theta}^\star) = L(\boldsymbol{\theta}^\star, \widehat{\boldsymbol{\theta}}^\star)$.

Therefore, the transformed model is equivalent to the standard sequence model with uncorrelated noise in Equation (4) and the estimation is equivalent to the estimation therein. Consequently, the ESD and span profile for the model in Equation (14) can be naturally defined using the original definitions for the transformed model. Specifically, for the correlated-noise model, we define the ESD w.r.t. $\boldsymbol{\Sigma}_\xi$ as

$$d_{\boldsymbol{\Sigma}_\xi}^\dagger (\tau; \boldsymbol{\theta}^\star) := d^\dagger \left(\tau; \tilde{\boldsymbol{\theta}}^\star = \mathbf{L}\boldsymbol{\theta}^\star \right)$$

Note that for the risk $\mathbb{E}L(\boldsymbol{\theta}^\star, \widehat{\boldsymbol{\theta}}^\star)$, our minimax risk characterization still applies, i.e., the minimax risk scales as $K\sigma^2$ across all distributions whose ESD $d_{\boldsymbol{\Sigma}_\xi}^\dagger \left(\sigma^2; \boldsymbol{\theta}^\star \right)$ is bounded by K.

The relationship between Euclidean distance and Mahalanobis distance satisfies that

$$\lambda_{\min}(\boldsymbol{\Sigma}_\xi) L(\boldsymbol{\theta}^\star, \widehat{\boldsymbol{\theta}}^\star) \leq \|\boldsymbol{\theta}^\star - \widehat{\boldsymbol{\theta}}^\star\|^2 \leq \lambda_{\max}(\boldsymbol{\Sigma}_\xi) L(\boldsymbol{\theta}^\star, \widehat{\boldsymbol{\theta}}^\star),$$

so the minimax risk in terms of $\mathbb{E}\|\boldsymbol{\theta}^\star - \widehat{\boldsymbol{\theta}}^\star\|^2$ can still be characterized sharply when the condition number of $\boldsymbol{\Sigma}_\xi$) is bounded.

This strategy of reducing a complex model to a simple model will be used in our analysis of linear model and also the RKHS regression in Section 8.

7.2 Linear Model

Consider the following fixed design linear regression model:

$$\mathbf{Y} = \mathbf{X}\boldsymbol{\beta}^* + \boldsymbol{\epsilon}, \tag{15}$$

where $\mathbf{Y} \in \mathbb{R}^n$ is the vector of observations, $\mathbf{X} \in \mathbb{R}^{n \times p}$ is the fixed design matrix of rank $r \leq \min(n, p)$, $\boldsymbol{\beta}^* \in \mathbb{R}^p$ is the unknown vector of true coefficients, and $\boldsymbol{\epsilon} \in \mathbb{R}^n$ is the noise vector. We assume the components of $\boldsymbol{\epsilon}$ are uncorrelated with mean zero and variance σ_0^2. For this model, we consider the loss (in-sample prediction error) $\mathcal{L}(\widehat{\boldsymbol{\beta}}; \boldsymbol{\beta}^*) = \frac{1}{n}\|\mathbf{X}\left(\widehat{\boldsymbol{\beta}} - \boldsymbol{\beta}^*\right)\|^2$ and risk $\mathcal{R}(\widehat{\boldsymbol{\beta}}; \boldsymbol{\beta}^*) = \mathbb{E}\mathcal{L}(\widehat{\boldsymbol{\beta}}; \boldsymbol{\beta}^*)$. For random design linear regression, we treat it as a special case of RKHS regression and discuss it in Section 8.

To connect this model to the sequence model analysis presented earlier, we utilize the Singular Value Decomposition (SVD) of the design matrix $\mathbf{X}$ as follows:

$$\frac{1}{\sqrt{n}}\mathbf{X} = \mathbf{U}\mathbf{S}\mathbf{V}^\top, \tag{16}$$

where $\mathbf{U} \in \mathbb{R}^{n \times n}$ and $\mathbf{V} \in \mathbb{R}^{p \times p}$ are orthogonal matrices, and $\mathbf{S} \in \mathbb{R}^{n \times p}$ is a rectangular diagonal matrix with non-negative singular values $s_1 \geq s_2 \geq \cdots \geq s_r > 0$ on its diagonal, and $s_j = 0$ for $j > r$.

For any matrix $\mathbf{A}$ and subsets R and T, we write $\mathbf{A}_{\cdot,R}$ for the submatrix formed by the columns of $\mathbf{A}$ with indices in R, and write $\mathbf{A}_{T,\cdot}$ for the submatrix formed by the rows of $\mathbf{A}$ with indices in T.

Multiplying the model Equation (15) by $\frac{1}{\sqrt{n}}\mathbf{U}_{\cdot,[r]}^\top$, we obtain a r-dimensional transformed model:

$$\mathbf{Z} = \boldsymbol{\theta}^* + \boldsymbol{\xi}, \tag{17}$$

where we have defined $\mathbf{Z} = \frac{1}{\sqrt{n}}\mathbf{U}_{\cdot,[r]}^\top\mathbf{Y}$, $\boldsymbol{\theta}^* = \frac{1}{\sqrt{n}}\mathbf{U}_{\cdot,[r]}^\top\mathbf{X}\boldsymbol{\beta}^* = \mathbf{S}_{[r],\cdot}\mathbf{V}^\top\boldsymbol{\beta}^*$, and $\boldsymbol{\xi} = \frac{1}{\sqrt{n}}\mathbf{U}_{\cdot,[r]}^\top\boldsymbol{\epsilon}$. Since $\mathbf{U}$ is orthogonal, the transformed noise vector $\boldsymbol{\xi}$ still has uncorrelated components with mean zero and variance $\sigma^2 := \sigma_0^2/n$.

The transformed model in Equation (17) is analogous to the sequence model in Equation (4), where the signal is $\boldsymbol{\theta}^*$ and the noise variance for each component is σ^2. The "spectrum" relevant to this problem is derived from the singular values of $\mathbf{X}$. Specifically, we define the eigenvalues as $\lambda_j = s_j^2$ for $j = 1, \ldots, r$, and $\lambda_j = 0$ for $j > r$. Let $\{\pi_k\}_{k=1}^r$ denote the indices corresponding to the eigenvalues sorted in descending order, $\lambda_{\pi_1} \geq \lambda_{\pi_2} \geq \cdots \geq \lambda_{\pi_r} > 0$.

For any estimator $\widehat{\boldsymbol{\beta}}$ for the linear model Equation (15), define $\widehat{\boldsymbol{\theta}} = \mathbf{S}_{[r],\cdot}\mathbf{V}^\top\widehat{\boldsymbol{\beta}}$. We can then write the prediction risk as $n^{-1}\mathbb{E}\|\mathbf{X}\widehat{\boldsymbol{\beta}} - \mathbf{X}\boldsymbol{\beta}^*\|^2 = \mathbb{E}\|\mathbf{U}\mathbf{S}\mathbf{V}^\top\widehat{\boldsymbol{\beta}} - \mathbf{U}\mathbf{S}\mathbf{V}^\top\boldsymbol{\beta}^*\|^2 = \mathbb{E}\|\widehat{\boldsymbol{\theta}} - \boldsymbol{\theta}^*\|^2$. Conversely, given an estimator $\widehat{\boldsymbol{\theta}}$ for the sequence model Equation (17), we can define $\widehat{\boldsymbol{\beta}} = \mathbf{V}\mathbf{S}^\dagger\widehat{\boldsymbol{\theta}}$ where $\mathbf{S}^\dagger \in \mathbb{R}^{p \times r}$ is an diagonal matrix whose diagonal elements are $\{1/s_j\}_{j \in [r]}$. It is easy to check that $\mathbf{S}_{[r],\cdot}\mathbf{V}^\top\widehat{\boldsymbol{\beta}} = \widehat{\boldsymbol{\theta}}$. Therefore, we establish an equivalence between the model Equation (17) and the model Equation (15).

The usual ridge regression estimator for the linear model Equation (15) is given by

$$\widehat{\boldsymbol{\beta}}_\nu = \left(\mathbf{X}^\top\mathbf{X} + \nu\,\mathbf{I}_p\right)^{-1}\mathbf{X}^\top\mathbf{Y},$$

which transforms into

$$\widehat{\boldsymbol{\theta}}_\nu = \mathbf{S}_{[r],\cdot}\mathbf{V}^\top\widehat{\boldsymbol{\beta}}_\nu = \left(\mathbf{I}_r - \psi_\nu(\mathrm{Diag}\,(\lambda_1, \ldots, \lambda_r))\right)\mathbf{Z}, \qquad \text{where } \psi_\nu(\lambda) = \frac{1}{\lambda/\nu + 1}.$$

13

In the above expression, we have used the identity that $\mathbf{S}_{[r],\cdot}\mathbf{S}_{[r],\cdot}^{\top} = \mathrm{Diag}\left(s_1^2, \ldots, s_r^2\right)$ and $\psi_\nu(\cdot)$ is applied element-wise. If we replace $\psi_\nu(\lambda)$ by other functions as discussed in Section 3, we recover other spectral methods.

7.3 ESD for linear models

We can now adapt the definitions from Section 3 to linear models.

Definition 7.1 (ESD for Linear Regression). *Suppose the SVD of the design matrix $\mathbf{X}$ is given in Equation (16). The Effective Span Dimension (ESD) of $\boldsymbol{\beta}^*$ with respect to the design $\mathbf{X}$ and the per component variance σ_0^2/n is defined as*

$$d^\dagger = d^\dagger(\sigma_0^2/n; \boldsymbol{\beta}^*, \mathbf{X}) = \min\{k \in [r] : \mathbf{H}_{\boldsymbol{\theta}^*, \boldsymbol{\lambda}}(k) \le \sigma_0^2/n\},$$

where $\boldsymbol{\theta}^* = \mathbf{S}_{\cdot,[r]}\mathbf{V}^{\top}\boldsymbol{\beta}^*$ and $\lambda_j = s_j^2$.

The Principal Component Regression (PCR) estimator for $\boldsymbol{\beta}^*$ corresponds to the Principal Component (PC) estimator in the transformed space Equation (17). Specifically, for any $k \in [r]$, define $\widehat{\boldsymbol{\beta}}^{\mathrm{PC},k} = \frac{1}{\sqrt{n}}\mathbf{V}\mathbf{S}_k^\dagger \mathbf{U}_{\cdot,[r]}^{\top}\mathbf{Y}$, where $\mathbf{S}_k^\dagger \in \mathbb{R}^{p \times r}$ is a diagonal matrix whose diagonal elements are $\{\frac{1}{s_j}\mathbf{1}_{\{s_j \ge s_{\pi_k}\}}\}$. In the $\mathbf{Z}$ space, this means

$$\hat{\theta}_j^{\mathrm{PC},k} = \mathbf{1}\{s_j \ge s_{\pi_k}\}Z_j, \quad j \in [r]. \tag{18}$$

Analogous to Theorem 3.2, the minimal prediction risk achievable by PCR over k is characterized by the ESD.

Proposition 7.2 (Optimal PCR Prediction Risk). *Let $\widehat{\boldsymbol{\beta}}^{\mathrm{PC},k}$ be the PCR estimator using the first k principal components. Let $\mathcal{R}_*^{\mathrm{PC}}$ be the minimal possible prediction risk over $k \in [r]$, i.e., $\mathcal{R}_*^{\mathrm{PC}} = \min_{k \in [r]} \mathcal{R}(\widehat{\boldsymbol{\beta}}^{\mathrm{PC},k}; \boldsymbol{\beta}^*)$. It holds that*

$$(d^\dagger - 1)\sigma_0^2/n \le \mathcal{R}_*^{\mathrm{PC}} \le 2d^\dagger\sigma_0^2/n,$$

where $d^\dagger = d^\dagger(\sigma_0^2/n; \boldsymbol{\beta}^*, \mathbf{X})$ is the ESD defined in Theorem 7.1.

Theorem 7.2 directly follows from Theorem 3.2 and its proof is omitted. This result shows that the optimal prediction risk for PCR is determined by the ESD $d^\dagger$, which measures the effective number of principal components needed to balance the bias-variance trade-off.

We can further extend the minimax analysis from Theorem 3.3. Let K be a quota on ESD. Define a class of coefficient vectors based on this quota:

$$\mathcal{B}_K^{(n)} = \left\{\boldsymbol{\beta} \in \mathbb{R}^p : d^\dagger(\sigma_0^2/n; \boldsymbol{\beta}^*, \mathbf{X}) \le K\right\}, \tag{19}$$

This class contains signals whose ESD relative to the design $\mathbf{X}$ is controlled by K. We can establish the minimax optimal rate for prediction over this class.

Theorem 7.3 (Minimax Prediction Risk for Linear Regression). *Suppose $K \le r$. For the linear model Equation (15) with noise variance σ_0^2, the minimax prediction risk over the class $\mathcal{B}_K^{(n)}$ defined in Equation (19) satisfies:*

$$\inf_{\widehat{\boldsymbol{\beta}}} \sup_{\boldsymbol{\beta}^* \in \mathcal{B}_K^{(n)}} \mathcal{R}(\widehat{\boldsymbol{\beta}}; \boldsymbol{\beta}^*) \asymp \sigma_0^2 \frac{K}{n}.$$

14

The proof of Theorem 7.3 is essentially the same as that of Theorem 3.3 and is omitted.

Through this extension, the span profile framework connects the optimal prediction performance in fixed design linear regression to the alignment between the signal structure (transformed via the design matrix) and the spectrum derived from the design matrix's singular values.

7.4 Numerical illustration

This section illustrates the ESD in fixed-design linear models in two examples. Throughout, we fix the noise variance at $\sigma_0^2 = 1$, the sample size at $n = 300$, and the dimension at $p = 400$.

Experimental set-up The baseline design matrix $\mathbf{X}_0$ is randomly generated with covariance matrix $\Sigma = \mathrm{Diag}\{\lambda_j\}_{j \in [p]}$ and then held fixed. We consider two cases:

1. *Geometric decay spectrum and polynomial decay signal*: $\lambda_j \propto 0.95^j$ and $\beta_j^* = j^{-0.2}$;

2. *Logarithmic decay spectrum and signal*: $\lambda_j = 1/\log(j+1)$ with $\beta_j^* = 1/\log(j+1)$.

The response will be generated from $\boldsymbol{Y} = \mathbf{X}_0 \boldsymbol{\beta}^* + \boldsymbol{\epsilon}$ with random noise $\boldsymbol{\epsilon}$.

We are interested in the ESD and the minimum risk for different transformation of the design matrix. For this purpose, we introduce a class of non-orthogonal column transformations indexed by $\alpha > 0$ as follows:

$$\mathbf{A}(\alpha) = \mathrm{diag}\big(\exp\{\alpha\, t_j\}\big), \quad t_j = (j-1)/(p-1) - 1/2, \quad j \in [p].$$

The transformed design $\mathbf{X}(\alpha) = \mathbf{X}_0 \mathbf{A}(\alpha)$ and the correspondingly transformed coefficient vector is $\boldsymbol{\beta}(\alpha) = \mathbf{A}(\alpha)^{-1} \boldsymbol{\beta}^*$. This family of transformation will change the order of spectrum, from well-aligned to misaligned. We are interested in the following at each α:

- Effective Span Dimension: $d^\dagger(\alpha) = d^\dagger\big(\sigma_0^2/n;\, \boldsymbol{\beta}(\alpha), \mathbf{X}(\alpha)\big)$;

- Minimal PCR risk: $\mathcal{R}_*(\alpha) = \min_k \mathbb{E}\big[n^{-1}\|\mathbf{X}(\alpha)\widehat{\boldsymbol{\beta}}_k - \mathbf{X}(\alpha)\boldsymbol{\beta}(\alpha)\|^2\big]$, where $\widehat{\boldsymbol{\beta}}_k$ is the k-component principal-component estimator based on $(\boldsymbol{Y}, \mathbf{X}(\alpha))$.

Figure 3 plots $d^\dagger(\alpha)$ (solid) and the rescaled oracle risk defined as $n\mathcal{R}_*(\alpha)/\sigma_0^2$ (dashed) against α. The two curves coincide over the entire path, which empirically verifies the bound in Theorem 7.2 that $\mathcal{R}_*(\alpha) \asymp \frac{\sigma_0^2}{n} d^\dagger(\alpha)$. As α grows, the diagonal stretch $\mathbf{A}(\alpha)$ shifts signal energy towards directions that carry smaller singular values. This raises $d^\dagger$ as well as the achievable risk increases.

This experiment illustrate that ESD, rather than the raw spectrum decay, is the pivotal measure that fully governs learnability.

8 Extension to RKHS Regression

This section extends the concepts of Effective Span Dimension (ESD) and span profile, developed in Section 3, to the setting of RKHS regression. Here we will focus on the simple case where the eigenfunctions of the kernel are fully known and computable and leave a thorough analysis in future studies.
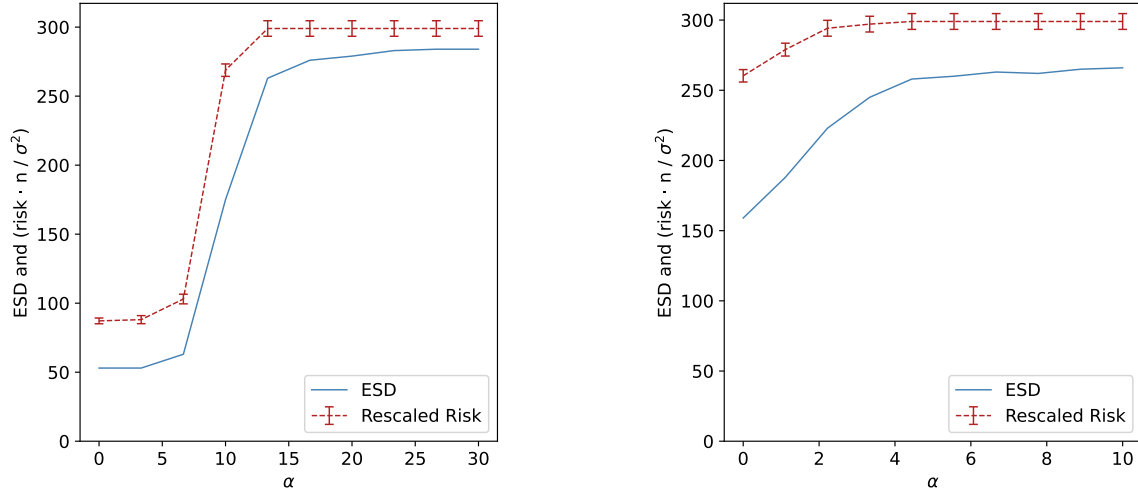
Figure 3: **Oracle PCR risk versus Effective Span Dimension** for (a) geometric eigen-decay and (b) logarithmic eigen-decay. The dashed line plots Risk $\times n/\sigma_0^2$; the solid line is $d^\dagger(\alpha)$. The risk is computed based on 20 replications and the error bar represents the standard deviation.

8.1 RKHS regression

We recall the standard random-design kernel regression model from Section 2:

$$y_i = f^*(x_i) + \epsilon_i, \quad \epsilon_i \overset{\text{i.i.d.}}{\sim} (0, \sigma_0^2), \quad i = 1, \dots, n, \tag{20}$$

where $x_i \sim \mu$ i.i.d., and $f^* \in L^2(\mathcal{X}, \mu)$ is the target function. We use a kernel $\mathbf{k}(\cdot, \cdot)$ with Mercer decomposition $\mathbf{k}(x, x') = \sum_{j=1}^{\infty} \lambda_j \psi_j(x) \psi_j(x')$, where $\{\psi_j\}_{j=1}^{\infty}$ form an orthonormal basis for $L^2(\mathcal{X}, \mu)$ and $\boldsymbol{\lambda} = \{\lambda_j\}_{j \geq 1}$ is the sequence of eigenvalues not necessarily sorted. For simplicity, we assume there is no ties among the eigenvalues and let π be the permutation sorting eigenvalues λ_j in descending order so that $\lambda_{\pi_1} > \lambda_{\pi_2} > \cdots > \lambda_{\pi_k} > \dots$. The coefficients of f^* in this basis are $\theta_j^* = \langle f^*, \psi_j \rangle_{L^2(\mu)}$. An estimator $\hat{f}$ has risk $\mathcal{R}(\hat{f}; f^*) = \mathbb{E}\|\hat{f} - f^*\|_{L^2(\mu)}^2$. If we define $\hat{\theta}_j = \langle \hat{f}, \psi_j \rangle_{L^2(\mu)}$, we can also write the risk as

$$\mathcal{R}(\hat{f}; f^*) = \mathbb{E}\|\hat{f} - f^*\|_{L^2(\mu)}^2 = \mathbb{E}\Big[\sum_{j=1}^{\infty} \left(\hat{\theta}_j - \theta_j^*\right)^2\Big] = \sum_{j=1}^{\infty} \mathbb{E}\left(\hat{\theta}_j - \theta_j^*\right)^2. \tag{21}$$

The expression in Equation (21) suggests that we can equivalently estimate each θ_j^* separately using the transformed observation $z_j = n^{-1} \sum_i y_i \psi_j(x_i)$ for any $j \geq 1$ as introduced in Equation (2).

Here we kindly remind the reader that in RKHS, we use to the subscript i to index samples while using j to index eigen-coordinates. The subscript j aligns with the use of notation in the sequence model, where we use indices j to denote coordinates.

Inflated variance in Equation (3). Before we introduce the definition of ESD, we demonstrate that the approximation in Equation (3) can be made exact by increasing the variance to encompass the approximation error.

16

For each $j \geq 1$, we can write the transformed observation as

$$
\begin{aligned}
z_j &= \frac{1}{n} \sum_{i=1}^n y_i \, \psi_j(x_i) \\
&= \frac{1}{n} \sum_{i=1}^n \left(f^*(x_i) + \epsilon_i \right) \psi_j(x_i) \\
&= \frac{1}{n} \sum_{i=1}^n \left(\sum_{k \geq 1} \theta_k^* \psi_k(x_i) \right) \psi_j(x_i) \; + \; \frac{1}{n} \sum_{i=1}^n \epsilon_i \, \psi_j(x_i) \\
&= \sum_{k \geq 1} \theta_k^* \underbrace{\left(\frac{1}{n} \sum_{i=1}^n \psi_k(x_i) \psi_j(x_i) \right)}_{:= G_{kj}} + \frac{1}{n} \sum_{i=1}^n \epsilon_i \, \psi_j(x_i) \\
&= \sum_{k \geq 1} G_{kj} \, \theta_k^* \; + \; \xi_j,
\end{aligned}
$$

where $G_{kj} := \frac{1}{n} \sum_{i=1}^n \psi_k(x_i) \psi_j(x_i)$ are entries of the empirical Gram matrix. For ξ_j, we have $\mathbb{E}(\xi_j \mid \{x_i\}_{i \in [n]}) = 0$ and $\mathbb{E}(\xi_j \xi_k \mid \{x_i\}_{i \in [n]}) = n^{-1} \sigma_0^2 G_{jk}$.

Since $x_i \overset{iid}{\sim} \mu$ and $\{\psi_j\}$ is orthonormal in $L^2(\mathcal{X}, \mu)$, then $\mathbb{E}[G_{kj}] = \mathbf{1}_{\{k=j\}}$. Hence $\mathbb{E}[z_j] = \theta_j^*$. We may further decompose z_j as follows

$$
z_j - \theta_j^* = (G_{jj} - 1)\theta_j^* + \left(\sum_{k \geq 1, k \neq j} G_{kj} \theta_k^* \right) + \xi_j = \Delta_j + \xi_j,
$$

where we have defined $\Delta_j = (G_{jj} - 1)\theta_j^* + \left(\sum_{k \geq 1, k \neq j} G_{kj} \theta_k^* \right)$. This term does not appear in the sequence model, and its randomness purely comes from random covariate x_i's. as $n \to \infty$, this term vanishes because $G_{jj} = n^{-1} \sum_i \psi_j(x_i)^2 \to 1$ and $G_{kj} = n^{-1} \sum_{i=1}^n \psi_j(x_i) \psi_{j'}(x_i) \to 0$. Furthermore, since $\mathbb{E}(\xi_j \mid \{x_i\}_{i \in [n]}) = 0$, we have

$$
\mathbb{E}(\Delta_j \xi_j) = \mathbb{E}(\Delta_j \mathbb{E}(\xi_j \mid \{x_i\}_{i \in [n]})) = 0.
$$

The presence of Δ_j effectively inflates the variance in z_j to $\sigma_0^2/n + \mathrm{Var}(\Delta_j)$. One can show that $\mathrm{Var}(\Delta_j) = \mathrm{Var}(f^*(x)\psi_j(x))$, which is bounded by $\|f\|_\infty^2$. This is how we will control the impact of Δ_j in the following development.

8.2 ESD for RKHS Regression

We start with analyzing the counterpart of the PC estimator, the Kernel Principal Component Projection Estimator (KPCPE), defined as

$$
\hat{f}^{\mathrm{PC},k}(x) := \sum_{j:\lambda_j \geq \lambda_{\pi_k}} z_j \psi_j(x), \tag{22}
$$

where k is the number of leading eigenfunctions to be included.

The risk $\mathcal{R}_k := \mathbb{E}\|\hat{f}_k^{\text{KPCPE}} - f^*\|_{L^2(\mu)}^2$ decomposes into squared bias $B(k)$ and variance $V(k)$. Since $\mathbb{E}[\psi_{j'}(x_i)\psi_j(x_i)] = 1_{\{j=j'\}}$, we have $\mathbb{E}[z_j] = \theta_j^*$. Therefore, the bias is due to truncation as

$$B(k) = \sum_{j=k+1}^{\infty} (\theta_j^*)^2. \tag{23}$$

The integrated variance is $V(k) = \sum_{j:\lambda_j \geq \lambda_{\pi_k}} \text{Var}(z_j)$. Using the law of total variance, we have

$$\text{Var}(z_j) = \frac{1}{n}\text{Var}(y_i\psi_j(x_i)) = \frac{1}{n}(\sigma_0^2 + \tau_j^2), \quad \text{where} \quad \tau_j^2 := \text{Var}(f^*(x)\psi_j(x)). \tag{24}$$

The term τ_j^2 arises from the randomness of the design x. To ensure $V(k)$ grows at the rate of k/n, we need to uniformly bound the design-induced variance τ_j^2. To illustrate the idea, we assume f^* is bounded in the sense that $|f^*(X)| \leq \|f^*\|_\infty$, μ-almost surely. Here, $\|f^*\|_\infty$ denotes the essential supremum of $|f^*|$ w.r.t. the measure μ.

Assumption 8.1 (Bounded target). *$f^* \in L^\infty(\mathcal{X}, \mu)$ and $\|f^*\|_\infty = \text{ess sup}\,|f^*|$.*

Theorem 8.1 is very mild: for compact $\mathcal{X}$, if f is continuous, then f is bounded.

Under Assumption 8.1, $\tau_j^2 \leq \mathbb{E}[f^*(x)^2\psi_j(x)^2] \leq \|f^*\|_\infty^2$. Subsequently, the variance is bounded by $V(k) \leq \frac{k}{n}(\sigma_0^2 + \|f^*\|_\infty^2)$. This motivates use to define the effective noise variance per component as

$$\sigma^2 := \frac{\sigma_0^2 + \|f^*\|_\infty^2}{n}. \tag{25}$$

The effective noise variance σ^2 includes the term $\|f^*\|_\infty^2/n$, which inflates the noise compared to an idealized sequence model.

We can now adapt the definitions from Section 3.1 using the effective noise variance σ^2.

Definition 8.2 (ESD for RKHS Regression). *The Effective Span Dimension (ESD) of f^* with respect to the kernel $\mathbf{k}$ and the effective noise variance $\sigma^2 = (\sigma_0^2 + \|f^*\|_\infty^2)/n$ is defined as*

$$d^\dagger = d^\dagger(\sigma^2; f^*, \mathbf{k}) = \min\{k \in \mathbb{N}_+ \cup \{\infty\} : \mathbf{H}_{\boldsymbol{\theta}^*, \boldsymbol{\lambda}}(k) \leq \sigma^2\}, \tag{26}$$

where $\boldsymbol{\theta}^* = \{\theta_j^*\}_{j\geq 1}$ and $\mathbf{H}_{\boldsymbol{\theta}^*, \boldsymbol{\lambda}}(k)$ is defined as in Equation (10).

The risk of the KPCPE estimator can be bounded using this ESD.

Proposition 8.3 (Optimal KPCPE Risk Bound). *Let $\hat{f}_k^{\text{PC}}$ be the KPCPE estimator defined in Equation (22). Let $\mathcal{R}_*^{\text{PC}} = \min_{k\geq 1} \mathcal{R}(\hat{f}_k^{\text{PC}}; f^*)$. Under Assumption 8.1, it holds that:*

$$(d^\dagger - 1)\frac{\sigma_0^2}{n} \leq \mathcal{R}_*^{\text{PC}} \leq 2d^\dagger\sigma^2 = 2d^\dagger\frac{\sigma_0^2 + \|f^*\|_\infty^2}{n}, \tag{27}$$

where $d^\dagger = d^\dagger(\sigma^2; f^*, \mathbf{k})$ is the ESD from Definition 8.2. In particular, if $\|f^*\|_\infty^2 \lesssim \sigma_0^2$, we can conclude that $\mathcal{R}_*^{\text{PC}} \asymp d^\dagger\sigma_0^2/n$.

We can also extend the minimax framework in Section 4 to RKHS regression. Let K be a quota on the ESD, and let C_0 be a constant. Define the class based on the span profile as follows:

$$\mathcal{F}_{K,\mathbf{k}}^{(n)} = \{f^* \in L^2(\mathcal{X}, \mu) \cap L^\infty(\mathcal{X}, \mu) : \|f^*\|_\infty \leq \sigma_0 C_0, \quad d^\dagger(\bar{\sigma}^2/n; f^*, \mathbf{k}) \leq K\}, \tag{28}$$

where $\bar{\sigma}^2 = \sigma_0^2(1 + C_0^2)$. We further impose the following assumption on the spectrum.

18

Assumption 8.4. *The kernel* **k** *is said to be* (K, n)-*regular if there are some constants* $c_1 < 1$ *and* C_1 *such that* $\sum_{i \leq c_1 K} \lambda_{\pi_i}^{-1} \leq C_1 n$.

Theorem 8.5 (Minimax Risk over Span Profile Classes)**.** *If* **k** *is* (K, n)-*regular, then the minimax risk over* $\mathcal{F}_{K,\mathbf{k}}^{(n)}$ *satisfies:*

$$\inf_{\hat{f}} \sup_{f^* \in \mathcal{F}_{K,\mathbf{k}}^{(n)}} \mathcal{R}(\hat{f}; f^*) \asymp \frac{\bar{\sigma}^2 K}{n}, \tag{29}$$

where the infimum is over all estimators $\hat{f}$.

Combining Theorem 8.5 and Theorem 8.3, the optimally tuned KPCPE estimator is minimax rate optimal over $\mathcal{F}_{K,\mathbf{k}}^{(n)}$, with rate $\bar{\sigma}_0^2 K/n$.

The KPCPE serves as a simple benchmark for spectral methods. This analysis, via the ESD, characterizes the performance of the optimally tuned KPCPE based directly on the properties of the specific signal f^* (via θ^*) and kernel spectrum λ, without requiring standard assumptions like source conditions or polynomial eigenvalue decay. Therefore, we consider the ESD evaluated at the design-adjusted noise level σ^2 as a key measure of statistical complexity in RKHS regression. In summary, the span profile framework provides a unified perspective on generalization performance of spectral methods on a variety of models.

Minimax convergence rates. Following the framework in Section 4, we can quantify a class of populations using a quota sequence $\mathbf{K} = \{K_n\}_{n=1}^{\infty}$. For some $n_0 \in \mathbb{N}_+$, define

$$\mathcal{F}_{\mathbf{K},\mathbf{k}} = \{f^* \in L^2(\mathcal{X}, \mu) \cap L^{\infty}(\mathcal{X}, \mu) : \|f^*\|_{\infty} \leq \sigma_0 C_0, \quad d^{\dagger}(\bar{\sigma}^2/n; f^*, \mathbf{k}) \leq K_n, \forall n \geq n_0\}, \tag{30}$$

where $\bar{\sigma}^2 = \sigma_0^2(1 + C_0^2)$. For a sample $\{(x_i, y_i)\}_{i=1}^{n}$ drawn from the model in Equation (20) and any estimator $\hat{f}$, we aim to determine the optimal convergence rate of the following minimax risk:

$$\inf_{\hat{f}} \sup_{f^* \in \mathcal{F}_{\mathbf{K},\mathbf{k}}} \mathcal{R}(\hat{f}, f^*). \tag{31}$$

We have the following result.

Theorem 8.6. *Suppose Theorem 4.1 holds for a quota sequence* $\boldsymbol{K} = \{K_n\}_{n=1}^{\infty}$. *Furthermore, suppose* **k** *is* (K_n, n)-*regular for all* $n \geq n_0$. *If* $\{(x_i, y_i)\}_{i=1}^{n}$ *is drawn from the model in Equation* (20), *it holds that*

$$\inf_{\hat{f}} \sup_{f^* \in \mathcal{F}_{\mathbf{K},\mathbf{k}}} \mathcal{R}(\hat{f}, f^*) \asymp \bar{\sigma}^2 \frac{K_n}{n}.$$

8.3 Connection to Random Design Linear Regression

The treatment of analysis developed in this section covers an important model, the random-design linear regression in contrast to the fixed-design linear regression. This is because linear regression can be viewed as a RKHS regression w.r.t. any positive definite linear kernels $\mathbf{k}(x, x') = x^{\top} \mathbf{K} x'$ for $x, x' \in \mathbb{R}^p$, where $\mathbf{K} \in \mathbb{R}^{p \times p}$ is positive definite.

Let the support $\mathcal{X}$ be a compact subset of $\mathbb{R}^p$. Suppose $\boldsymbol{\Sigma}_x = \mathbb{E}_{x\sim\mu}(xx^\top)$ is positive definite and $\mathbf{L}$ is a symmetric square root of $\boldsymbol{\Sigma}_x$. Let the eigen-decomposition of $\mathbf{LKL}$ be

$$\mathbf{LKL} = \sum_{j=1}^p \lambda_j v_j v_j^\top = \mathbf{V\Lambda V}^\top,$$

where $\mathbf{V}$ is the matrix with columns formed by v_j and $\boldsymbol{\Lambda} = \mathrm{Diag}(\ldots \lambda_i \ldots)$.

Define $\boldsymbol{\Psi} = \mathbf{L}^{-1}\mathbf{V}$. Then $\boldsymbol{\Psi}^\top \boldsymbol{\Sigma}_x \boldsymbol{\Psi} = \mathbf{V}^\top \mathbf{V} = \mathbf{I}_p$. Furthermore, we have

$$\mathbf{K} = \mathbf{L}^{-1}\mathbf{V\Lambda V}^\top \mathbf{L}^{-1} = \boldsymbol{\Psi\Lambda\Psi}^\top,$$

Suppose the columns of $\boldsymbol{\Psi}$ are ψ_j. We can then write

$$\mathbb{E}_{x\sim\mu}\left[\langle\psi_j, x\rangle\langle\psi_j, x\rangle\right] = \left(\boldsymbol{\Psi}^\top\boldsymbol{\Sigma}_x\boldsymbol{\Psi}\right)_{jk} = \mathbf{1}_{\{j=k\}}, \quad \forall j, k \in [p],$$

so $\{\psi_j\}$ is an orthonormal system in $L^2(\mathcal{X}, \mu)$. Furthermore, the kernel can be expressed as

$$\mathbf{k}(x, x') = x^\top \mathbf{K} x' = \sum_{j=1}^p \lambda_j \langle\psi_j, x\rangle\langle\psi_j, x'\rangle.$$

Hence, $(\{\lambda_i\}, \{\psi_j\})$ is the eigen-pair for $\mathbf{k}$.

For linear regression where $y = f^*(x) + \epsilon$ and $f^*(x) = \langle\beta^*, x\rangle$. Define $\theta^* = \boldsymbol{\Psi}^{-1}\beta^* = \mathbf{V}^\top \mathbf{L}\beta^*$. We can write

$$f^*(x) = \langle\beta^*, x\rangle = \langle\boldsymbol{\Psi}^{-1}\beta^*, \boldsymbol{\Psi}^\top x\rangle = \sum_{j=1}^p \theta_j^* \langle\psi_j, x\rangle.$$

It is also clear that $\|f^*\|_\infty \le \sup_{x\in\mathcal{X}}\langle\beta^*, x\rangle \le \|\beta^*\|_2 C_\mathcal{X} < \infty$, where $C_\mathcal{X}$ is finite and depends on $\mathcal{X}$. We can define the effective noise level $\sigma^2 = n^{-1}(\sigma_0^2 + \|f^*\|_\infty^2)$.

Therefore, with respect to the kernel $\mathbf{k}$ and the basis $\{\psi_j\}$, we define the ESD exactly as in Theorem 8.2 using the coefficients $\{\theta_j^*\}$ and eigenvalues $\{\lambda_j\}$.

8.4   Numerical Illustration

This section provides numerical validation of the relationship between the ESD and the optimally tuned KPCPE risk, mirroring the setup for linear models in Section 7.4. We use the cosine basis eigenfunctions $\psi_j(x) = \sqrt{2}\cos(2\pi j x)$ on the domain $[0, 1]$ with inputs sampled as $x_i \overset{\text{i.i.d.}}{\sim} \mathrm{Unif}[0, 1]$. The sample size is fixed at $n = 400$, and for numerical purpose, we consider the first $J = 800$ eigenfunctions. The noise variance is set as $\sigma_0^2 = 1$.

Experimental Setup: We set the baseline kernel eigenvalue spectrum as $\lambda_{j,0} = j^{-1.1}$ and the fixed signal coefficients as $\theta_j^* = j^{-4}$. To study the impact of misalignment between the kernel spectrum and the signal, we introduce a severity parameter $\alpha \ge 0$ and define the modified eigenvalue spectrum as

$$\lambda_j(\alpha) = \lambda_{j,0}\exp\left(\alpha t_j\right), \quad t_j = \frac{j-1}{D-1} \text{ for } j \le D, \text{ and } t_j = 0 \text{ otherwise,}$$

with $D = 80$. As α increases, the leading D eigenvalues become progressively magnified, with the largest index having the most significant increase. Consequently, the modified kernel will emphasize more on directions that received less energy of the signal and the optimal KPCPE should require selecting more principal components.

As the severity parameter α grows, only the first D eigenvalues are changed while the rest of the spectrum is untouched. Among the changed ones, the leading eigenvalues are magnified by a smaller constant, so that the resulting kernel has its leading subspaces being on the directions in which the signal has less of its energy and thus increases the misalignment.

For each α in a specified grid, we compute two quantities:

- The Effective Span Dimension

$$d_{\text{eff}}^{\dagger}(\alpha) = d^{\dagger}\left(\sigma_{\text{eff}}^2; f^*, \lambda(\alpha)\right), \quad \sigma_{\text{eff}}^2 := \frac{\sigma_0^2 + \sigma_{f,4}^2}{n},$$

where the design-induced variance $\sigma_{f,4}^2 = \max_{j \leq J} \text{Var}\left\{f^*(X)\psi_j(X)\right\}$ is computed numerically based on the fixed sample of x_i and the true f^*.

- The optimally tuned KPCPE risk

$$\mathcal{R}_*(\alpha) = \min_k \mathbb{E}\|\hat{f}_k^{\text{PC}}(\alpha) - f^*\|_{L^2(\mu)}^2,$$

where the estimator $\hat{f}_k^{\text{PC}}(\alpha)$ is computed using the spectrum $\lambda(\alpha)$ and the expectation is estimated by averaging prediction error over $B = 10$ Monte Carlo replications.
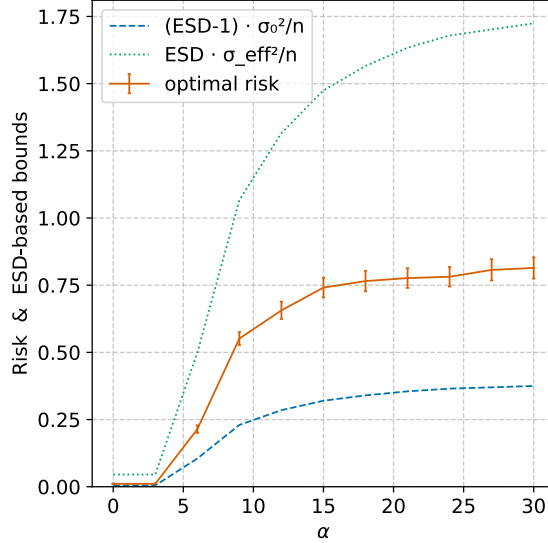

Figure 4: Effective Span Dimension and Optimal KPCPE risk. The dashed line plots Risk $\times n/\sigma_0^2$; the solid line is $d^{\dagger}(\alpha)$. The risk is computed based on 20 replications and the error bar represents the standard deviation.

Figure 4 plots the empirically computed optimal KPCPE risk (orange solid line) alongside the theoretical lower bound $(d^{\dagger} - 1)\sigma_0^2/n$ (blue dashed line) and upper bound $2d^{\dagger}\sigma_{\text{eff}}^2$ (green

21

dotted line). The empirical risk consistently lies between the two theoretical curves, confirming the validity of the bounds derived in Proposition 8.3.

As the severity parameter α increases, the resulting spectral perturbation shifts energy into higher-index eigenfunctions. This inflates the ESD and consequently the minimal achievable risk.

Overall, this experiment demonstrates that our span profile framework provides an accurate and robust characterization of generalization performance in RKHS regression, consistent with earlier observations made for the sequence and linear regression models.

9 Measuring Alignment via ESD

We illustrate how the notion of ESD can be used to measure the alignment between the signal and the kernel (spectrum).

9.1 An example of comparing signal-spectrum alignments

The following is a simple example to illustrate the idea of comparing the signal-spectrum alignments for different spectra discussed in Section 3.2.

Suppose $\boldsymbol{\theta}^*$ is s-sparse with support $S \subset [d]$ and $s = |S| \ll d$. Consider the following two spectra with the same set of eigenvalues but different allocations:

(1) The first k largest eigenvalues of $\boldsymbol{\lambda}^{(1)}$ are located on S;
(2) The first k largest eigenvalues of $\boldsymbol{\lambda}^{(2)}$ are located on $S^c = [d] \setminus S$.

Intuitively, $\boldsymbol{\lambda}^{(1)}$ aligns better with $\boldsymbol{\theta}^*$ than $\boldsymbol{\lambda}^{(2)}$. However, a quantitative analysis is not obvious without using the notion of ESD.

Firstly, we note that the effective dimensions [51] for these two spectra are the same because the sets of eigenvalues are the same. Similarly, the covariance splitting indices k^* [5] are the same for the two spectra. We confirm that signal-agnostic complexity measures do not distinguish the signal-spectrum alignments for these two spectra.

Next, we consider the ESD and span profile. Rigorously, we can show for any τ,

$$\mathbf{D}_{\boldsymbol{\theta}^*, \boldsymbol{\lambda}^{(1)}}(\tau) \leq s, \text{ and } \mathbf{D}_{\boldsymbol{\theta}^*, \boldsymbol{\lambda}^{(2)}}(\tau) \geq \min\left(d - s, \|\boldsymbol{\theta}^*\|^2/\tau\right).$$

Hence, for sufficiently small τ, their ratio

$$r(\tau) = \mathbf{D}_{\boldsymbol{\theta}^*, \boldsymbol{\lambda}^{(1)}}(\tau)/\mathbf{D}_{\boldsymbol{\theta}^*, \boldsymbol{\lambda}^{(2)}}(\tau) \leq s/(d - s) \ll 1$$

In view of Theorem 3.3, this suggests that the minimax estimation using $\boldsymbol{\lambda}^{(1)}$ is substantially than using $\boldsymbol{\lambda}^{(2)}$ when the noise level is small. Therefore, spectral estimators using $\boldsymbol{\lambda}^{(1)}$ is preferred.

9.2 Pathwise ESD for Learned Kernels

Section 5 analyzes eigenvalue learning because OP-GF admits tractable dynamics under a fixed eigenbasis. This is a limitation of that specific analysis, not of the ESD concept. In fact, ESD applies to general representation learning. We illustrate how decreases in ESD explain

minimax risk reduction for learned kernels, whether adaptation acts through eigenvalues, eigenfunctions, or both.

Let $\mathbf{k}_t$ be the kernel learned at training time t, with eigenvalues $\{\lambda_j(t)\}$ (sorted decreasing) and $L^2(\mathcal{X}, \mu)$-orthonormal eigenfunctions $\{\psi_j^{(t)}\}$. To understand how the signal-kernel alignment evolves, we define the pathwise ESD as

$$d^\dagger(t) := d^\dagger(\sigma^2; f^*, \mathbf{k}_t), t \geq 0,$$

where we have followed Theorem 8.2 to define $d^\dagger(\sigma^2; f^*, \mathbf{k}_t)$ as the ESD of f^* w.r.t. the kernel $\mathbf{k}_t$ using $\theta_j^{*,(t)} = \langle f^*, \psi_j^{(t)} \rangle$ and $\sigma^2 = n^{-1}(\sigma_0^2 + \|f^*\|_\infty^2)$.

Let $\mathbf{H}_t(k) := \frac{1}{k} \sum_{i>k} \left[\theta_i^{*,(t)}\right]^2$. If training aligns the leading eigenfunctions $\psi_j^{(t)}$ better with f^*, then $\{\theta_j^{*,(t)}\}$ concentrate more on leading indices, and thus $\mathbf{H}_t(k)$ decreases for all k, which implies the decrease in $d^\dagger(t)$.

Experiment on Deep Linear Networks. To demonstrate this pathwise perspective, we simulate a random-design linear regression.

Each covariate coordinate is drawn independently from $\{\pm 1\}$, so $\mathbf{\Sigma}_x = \mathbb{E}(XX^\top) = \mathbf{I}_p$ and $\|X\|_\infty = 1$. We set $p = 900$, and the true parameters are set as follows: β^* follows a power-law decay with $\beta_j^* = j^{-1.1}$ for $1 \leq j \leq 200$ and $\beta_j^* = 0$ for $j > 200$. The response is $Y = \langle \beta^*, X \rangle + \varepsilon$ with $\varepsilon \sim N(0, \sigma_0^2)$ and $\sigma_0 = 0.1$.

We draw $n = 1000$ samples and train a deep *linear network* with $D = 4$ hidden affine maps without bias using full-batch Adam with learning rate 10^{-4}. The hidden weight matrices of the network are $\mathbf{W}_\ell(t) \in \mathbb{R}^{p \times p}$ for $\ell = 1, \ldots, D$ (using a near-identity initialization) and the weight of a final linear layer is $w(t) \in \mathbb{R}^p$.

The estimated function at time t is given by $f_t(x) = w(t)^\top \mathbf{A}(t) x$, where $\mathbf{A}(t) := \mathbf{W}_D(t) \cdots \mathbf{W}_1(t)$. We form the learned kernel $\mathbf{k}_t(x, x') = \langle \mathbf{A}(t)x, \mathbf{A}(t)x' \rangle = x^\top \mathbf{G}_t x'$ where $G_t := \mathbf{A}(t)_t^\top \mathbf{A}(t)_t$. We then follow the derivation in Section 8.3 and define the ESD $d^\dagger(t)$ of f^* w.r.t. the kernel $\mathbf{k}_t$. Since $\|X\|_\infty = 1$ μ-a.s., we have $\|f\|_\infty^2 = \|\beta\|_1^2 = \|\beta\|_1^2$; this is used in computing the effective noise level.

Figure 5 shows that adaptive representation learning progressively reduces the ESD $d^\dagger(t)$ in t along with the true risk. This confirms that ESD captures the evolving alignment between signal and kernel.

10   Discussion

This paper introduces the effective span dimension (ESD) and span profile to analyze the interplay between the signal structure and the kernel spectrum. Our framework moves beyond classical static assumptions relative to a fixed kernel (e.g., source conditions and polynomial eigenvalue decay) and offers a dynamic, noise-dependent perspective on signal complexity. Unlike traditional source conditions, the ESD is more flexible and remains applicable when the spectrum itself is learned from data.

Quantifying adaptivity. Like the sparsity level in high-dimensional statistics, the ESD is a population quantity for theoretical analyses rather than an input to training. It serves as a quantitative target for adaptive algorithms on the population level: by comparing the ESD
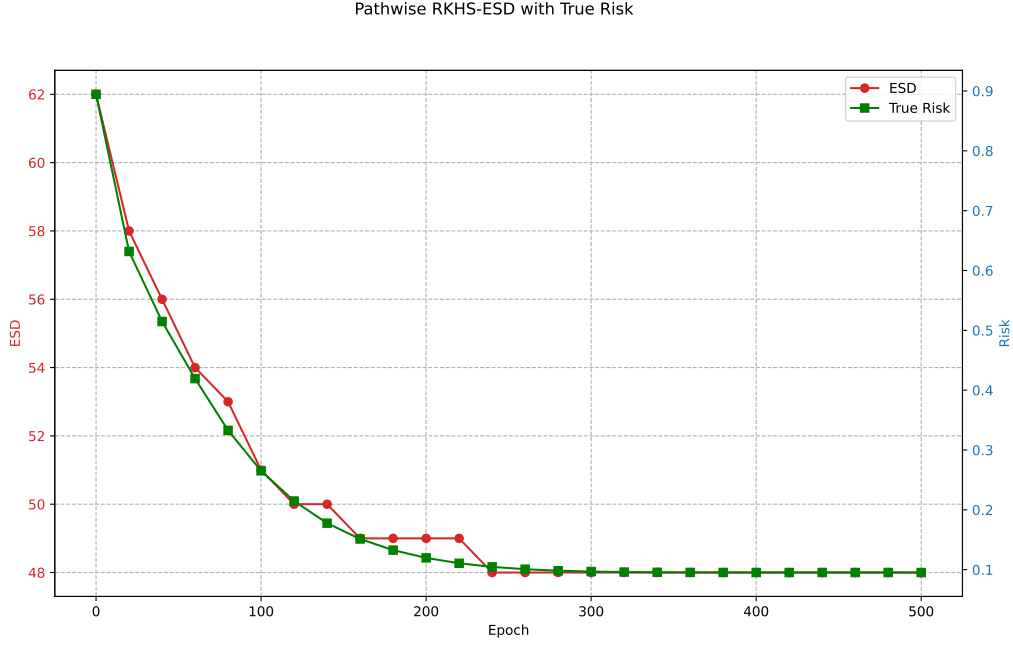
Figure 5: Pathwise ESD and risk under a learned kernel using a 4-layer linear network.

of a particular signal w.r.t. different kernels, we can determine which kernel permits better generalization for this signal.

Connecting adaptivity and generalization. Our span profile framework clarifies why adaptive machine learning methods often outperform classical fixed-kernel approaches. In classical methods with a fixed kernel spectrum $\boldsymbol{\lambda}^{(0)}$, the target signal $\boldsymbol{\theta}^*$ might exhibit poor alignment, resulting in a large span profile $D_{\boldsymbol{\theta}^*, \boldsymbol{\lambda}^{(0)}}$. Consequently, the signal resides in a class $\mathcal{F}_{\mathbf{K}^{(0)}, \boldsymbol{\lambda}^{(0)}}$ with a large quota sequence $\mathbf{K}^{(0)}$, which implies high minimax risk. By contrast, adaptive methods modify the kernel during training. Successful adaptation improves the alignment by reducing the span profile $D_{\boldsymbol{\theta}^*, \boldsymbol{\lambda}^{(a)}}$ of the same signal w.r.t. the adapted kernel spectrum $\boldsymbol{\lambda}^{(a)}$. This adaptation places the signal in a class $\mathcal{F}_{\mathbf{K}^{(a)}, \boldsymbol{\lambda}^{(a)}}$ with a smaller quota sequence $\mathbf{K}^{(a)}$, which implies lower minimax risk.

In summary, the ESD framework provides a novel view of generalization that connects classical kernel methods with modern adaptive learning. We expect to relate this framework to learned representations in neural networks to explain their superior generalization performance.

References

[1] A. Agarwal, D. Shah, D. Shen, and D. Song. On robustness of principal component regression. *Advances in Neural Information Processing Systems*, 32, 2019.

[2] Z. Allen-Zhu, Y. Li, and Z. Song. A convergence theory for deep learning via over-parameterization, June 2019. URL `http://arxiv.org/abs/1811.03962`.

[3] S. Arora, S. Du, W. Hu, Z. Li, and R. Wang. Fine-grained analysis of optimization

and generalization for overparameterized two-layer neural networks. In *International Conference on Machine Learning*, pages 322–332. PMLR, 2019.

[4] J. Ba, M. A. Erdogdu, T. Suzuki, Z. Wang, D. Wu, and G. Yang. High-dimensional asymptotics of feature learning: How one gradient step improves the representation, May 2022.

[5] P. L. Bartlett, P. M. Long, G. Lugosi, and A. Tsigler. Benign overfitting in linear regression. *Proceedings of the National Academy of Sciences*, 117(48):30063–30070, Dec. 2020. ISSN 0027-8424, 1091-6490. doi: 10.1073/pnas.1907378117.

[6] P. L. Bartlett, P. M. Long, G. Lugosi, and A. Tsigler. Benign overfitting in linear regression. *Proceedings of the National Academy of Sciences*, 117(48):30063–30070, 2020.

[7] D. Barzilai and O. Shamir. Generalization in kernel regression under realistic assumptions. *arXiv preprint arXiv:2312.15995*, 2023.

[8] F. Bauer, S. Pereverzev, and L. Rosasco. On regularization algorithms in learning theory. *Journal of complexity*, 23(1):52–72, 2007. doi: 10.1016/j.jco.2006.07.001.

[9] X. Bing, F. Bunea, S. Strimas-Mackey, and M. Wegkamp. Prediction under latent factor regression: Adaptive pcr, interpolating predictors and beyond. *Journal of Machine Learning Research*, 22(177):1–50, 2021.

[10] B. Bordelon, A. Atanasov, and C. Pehlevan. How feature learning can improve neural scaling laws. In *The Thirteenth International Conference on Learning Representations*, 2025. URL https://openreview.net/forum?id=dEypApI1MZ.

[11] L. D. Brown, T. T. Cai, M. G. Low, and C.-H. Zhang. Asymptotic equivalence theory for nonparametric regression with random design. *The Annals of Statistics*, 30(3):688–707, 2002. ISSN 0090-5364. doi: 10.1214/aos/1028674838.

[12] A. Caponnetto and E. D. Vito. Optimal rates for the regularized least-squares algorithm. *Foundations of Computational Mathematics*, 7(3):331–368, 2007.

[13] C. Cortes, M. Mohri, and A. Rostamizadeh. Algorithms for learning kernels based on centered alignment. *The Journal of Machine Learning Research*, 13(1):795–828, 2012.

[14] N. Cristianini, J. Shawe-Taylor, A. Elisseeff, and J. Kandola. On kernel-target alignment. *Advances in neural information processing systems*, 14, 2001.

[15] H. W. Engl, M. Hanke, and A. Neubauer. *Regularization of Inverse Problems*, volume 375. Springer Science & Business Media, 1996.

[16] K. Gatmiry, S. Jegelka, and J. Kelner. Optimization and Adaptive Generalization of Three layer Neural Networks. In *International Conference on Learning Representations*, Oct. 2021. URL https://openreview.net/forum?id=dPyRNUlttBv.

[17] D. Gedon, A. H. Ribeiro, and T. B. Schön. No double descent in principal component regression: A high-dimensional analysis. In *Forty-first International Conference on Machine Learning*, 2024.

[18] L. L. Gerfo, L. Rosasco, F. Odone, E. D. Vito, and A. Verri. Spectral algorithms for supervised learning. *Neural Computation*, 20(7):1873–1897, 2008.

[19] B. Ghorbani, S. Mei, T. Misiakiewicz, and A. Montanari. When do neural networks outperform kernel methods? *Advances in Neural Information Processing Systems*, 33: 14820–14830, 2020.

[20] A. Green and E. Romanov. The high-dimensional asymptotics of principal component regression. *arXiv preprint arXiv:2405.11676*, 2024.

[21] N. T. Huang, D. W. Hogg, and S. Villar. Dimensionality reduction, regularization, and generalization in overparameterized regressions. *SIAM Journal on Mathematics of Data Science*, 4(1):126–152, 2022.

[22] L. Hucker and M. Wahl. A note on the prediction error of principal component regression in high dimensions. *Theory of Probability and Mathematical Statistics*, 109:37–53, 2023.

[23] A. Jacot, F. Gabriel, and C. Hongler. Neural tangent kernel: Convergence and generalization in neural networks. In S. Bengio, H. Wallach, H. Larochelle, K. Grauman, N. Cesa-Bianchi, and R. Garnett, editors, *Advances in Neural Information Processing Systems*, volume 31. Curran Associates, Inc., 2018. URL `https://proceedings.neurips.cc/paper/2018/file/5a4be1fa34e62bb8a6ec6b91d2462f5a-Paper.pdf`.

[24] I. M. Johnstone. Gaussian estimation: Sequence and wavelet models. 2017.

[25] S. Karp, E. Winston, Y. Li, and A. Singh. Local signal adaptivity: Provable feature learning in neural networks beyond kernels. *Advances in Neural Information Processing Systems*, 34:24883–24897, 2021.

[26] S. Kornblith, M. Norouzi, H. Lee, and G. Hinton. Similarity of neural network representations revisited. In *International conference on machine learning*, pages 3519–3529. PMLR, 2019.

[27] D. Kunin, A. Raventós, C. Dominé, F. Chen, D. Klindt, A. Saxe, and S. Ganguli. Get rich quick: exact solutions reveal how unbalanced initializations promote rapid feature learning. *Advances in Neural Information Processing Systems*, 37:81157–81203, 2024.

[28] Y. Li and Q. Lin. Improving adaptivity via over-parameterization in sequence models. In *The Thirty-eighth Annual Conference on Neural Information Processing Systems*, 2024. URL `https://openreview.net/forum?id=UfLH4T676K`.

[29] Y. Li and Q. Lin. Diagonal over-parameterization in reproducing kernel hilbert spaces as an adaptive feature model: Generalization and adaptivity. *arXiv preprint arXiv:2501.08679*, 2025.

[30] Y. Li, W. Gan, Z. Shi, and Q. Lin. Generalization error curves for analytic spectral algorithms under power-law decay. *arXiv preprint arXiv:2401.01599*, 2024.

[31] Y. H. Liu, A. Baratin, J. Cornford, S. Mihalas, E. T. SheaBrown, and G. Lajoie. How connectivity structure shapes rich and lazy learning in neural circuits. In *The Twelfth International Conference on Learning Representations*, 2024.

[32] P. Mathé and S. V. Pereverzev. Geometry of linear ill-posed problems in variable hilbert scales. *Inverse problems*, 19(3):789, 2003.

[33] A. Radhakrishnan, D. Beaglehole, P. Pandit, and M. Belkin. Mechanism for feature learning in neural networks and backpropagation-free machine learning models. *Science*, 383(6690):1461–1467, 2024.

[34] L. Rosasco, E. De Vito, and A. Verri. Spectral methods for regularization in learning theory. *DISI, Universita degli Studi di Genova, Italy, Technical Report DISI-TR-05-18*, 2005.

[35] B. Schölkopf and A. J. Smola. *Learning with Kernels: Support Vector Machines, Regularization, Optimization, and Beyond.* MIT Press, 2002.

[36] M. Seleznova and G. Kutyniok. Analyzing finite neural networks: Can we trust neural tangent kernel theory? In *Mathematical and Scientific Machine Learning*, pages 868–895. PMLR, 2022. URL `https://proceedings.mlr.press/v145/seleznova22a.html`.

[37] Z. Shi, J. Wei, and Y. Liang. Provable guarantees for neural networks via gradient feature learning. *Advances in Neural Information Processing Systems*, 36:55848–55918, 2023.

[38] I. Steinwart and A. Christmann. *Support vector machines.* Springer Science & Business Media, 2008.

[39] I. Steinwart and C. Scovel. Mercer's Theorem on General Domains: On the Interaction between Measures, Kernels, and RKHSs. 2012. doi: 10.1007/S00365-012-9153-3.

[40] A. Tsigler and P. L. Bartlett. Benign overfitting in ridge regression. *Journal of Machine Learning Research*, 24(123):1–76, 2023.

[41] G. Wahba. *Spline Models for Observational Data*, volume 59 of *CBMS-NSF Regional Conference Series in Applied Mathematics.* SIAM, 1990.

[42] C. Wang, X. He, Y. Wang, and J. Wang. On the target-kernel alignment: a unified analysis with kernel complexity. *Advances in Neural Information Processing Systems*, 37: 40434–40485, 2024.

[43] J. Wenger, F. Dangel, and A. Kristiadi. On the disconnect between theory and practice of overparametrized neural networks, Sept. 2023. URL `http://arxiv.org/abs/2310.00137`.

[44] B. Woodworth, S. Gunasekar, J. D. Lee, E. Moroshko, P. Savarese, I. Golan, D. Soudry, and N. Srebro. Kernel and rich regimes in overparametrized models. In *Proceedings of Thirty Third Conference on Learning Theory*, pages 3635–3673. PMLR, July 2020. URL `https://proceedings.mlr.press/v125/woodworth20a.html`.

[45] D. Wu and J. Xu. On the optimal weighted ℓ_2 regularization in overparameterized linear regression. *Advances in Neural Information Processing Systems*, 33:10112–10123, 2020.

[46] J. Xu and D. J. Hsu. On the number of variables to use in principal component regression. *Advances in neural information processing systems*, 32, 2019.

[47] Y. Xu and L. Ziyin. Three mechanisms of feature learning in a linear network. In *The Thirteenth International Conference on Learning Representations*, 2025.

[48] Y. Yao, L. Rosasco, and A. Caponnetto. On early stopping in gradient descent learning. *Constructive Approximation*, 26:289–315, Aug. 2007. doi: 10.1007/s00365-006-0663-2.

[49] B. Yu. Assouad, fano, and le cam. In *Festschrift for Lucien Le Cam: research papers in probability and statistics*, pages 423–435. Springer, 1997.

[50] H. Zhang, J. Lai, Y. Li, Q. Lin, and J. S. Liu. Towards a statistical understanding of neural networks: Beyond the neural tangent kernel theories. *arXiv preprint arXiv:2412.18756*, 2024.

[51] T. Zhang. Learning bounds for kernel regression using effective data dimensionality. *Neural Computation*, 17(9):2077–2098, 2005. doi: 10.1162/0899766054323008.

A Proof

A.1 Proofs of Results on ESD of Sequence Models

Proof of Theorem 3.2. For any $\nu > 0$, define

$$k_\Lambda(\nu) = \#\{\,j : \lambda_j \geq \nu\,\},$$

which counts how many eigenvalues exceed the threshold ν. The KPCR estimator sets

$$\hat{\theta}_i^\nu = 1_{\{\lambda_i \geq \nu\}}\, z_i,\ i \in [d].$$

Its squared bias and variance are given by

$$B^{\mathrm{PC}}(v) = \sum_{i:\lambda_i < v} (\theta_i^*)^2,\ V^{\mathrm{PC}}(v) = \sum_{i:\lambda_i \geq v} \sigma^2 = k_\Lambda(v)\,\sigma^2.$$

For any threshold v, we can reparameterize the bias and variance using $k = k_\Lambda(v)$ as

$$B^{\mathrm{PC}}(k) = \sum_{i=k+1}^{d} \left(\theta_{\pi_i}^*\right)^2,\quad \text{and}\quad V^{\mathrm{PC}}(k) = k\,\sigma^2, k = 0, 1, \ldots, d.$$

The function $B^{\mathrm{PC}}(k)$ decreases in k, while $V^{\mathrm{PC}}(k)$ increases in k. The risk function is given by $\mathcal{R}^{\mathrm{PC}}(k) = B^{\mathrm{PC}}(k) + V^{\mathrm{PC}}(k)$.

For any integer $k \geq 1$, we have

$$\mathcal{R}^{\mathrm{PC}}(k) = k\left(\sigma^2 + \frac{1}{k}\sum_{i:\lambda_i < \lambda_{\pi_k}} (\theta_i^*)^2\right).$$

Upper bound For $k = d^\dagger$, we have $\frac{1}{k}\sum_{i:\lambda_i < \lambda_{\pi_k}} (\theta_i^*)^2 \leq \sigma^2$. By definition of the optimal risk, we have

$$\mathcal{R}_*^{\mathrm{PC}} \leq \mathcal{R}^{\mathrm{PC}}(d^\dagger) \leq 2\,d^\dagger \sigma^2.$$

Therefore, the upper bound is proved.

Lower bound Without loss of generality, assume $d^\dagger \geq 2$. For any $k \leq d^\dagger - 1$, we have

$$\mathcal{R}^{\mathrm{PC}}(k) \geq B^{\mathrm{PC}}(k) = \sum_{i=k+1}^{d} \left(\theta_{\pi_i}^*\right)^2 \geq \sum_{i=d^\dagger}^{d} \left(\theta_{\pi_i}^*\right)^2 > (d^\dagger - 1)\sigma^2,$$

where the last inequality comes from the definition of $d^\dagger$. For any $k \in [d^\dagger, d]$, we have

$$\mathcal{R}^{\mathrm{PC}}(k) \geq k\sigma^2 \geq d^\dagger \sigma^2.$$

Therefore, the lower bound is proved. □

A.2 Proof on Minimax Results

Proof of Theorem 4.3. Throughout the proof, the quota sequence is fixed. Recall the definition of M_k in Theorem 4.1. Define $\psi(k) = \sigma_0^2 \frac{k}{M_k}$ for any $k \in \bar{K}$. Also define $\mathbf{S}_{\boldsymbol{\theta},\boldsymbol{\lambda}}(k) = k \mathbf{H}_{\boldsymbol{\theta},\boldsymbol{\lambda}}(k)$.

We can express $\mathcal{F}_{\boldsymbol{K},\boldsymbol{\lambda}}$ as follows.

Lemma A.1. *Under Theorem 4.1, we have*

$$\mathcal{F}_{\boldsymbol{K},\boldsymbol{\lambda}} = \left\{ \boldsymbol{\theta} \in \mathbb{R}^\infty : \mathbf{S}_{\boldsymbol{\theta},\boldsymbol{\lambda}}(k) \leq \psi(k) \text{ for all } k \in [\bar{K}] \right\}.$$

Proof of Theorem A.1. Observe the relation that

$$\boldsymbol{\theta} \in \mathcal{F}_{\boldsymbol{K},\boldsymbol{\lambda}} \iff \mathbf{D}_{\boldsymbol{\theta},\boldsymbol{\lambda}}\left(\frac{\sigma_0^2}{n}\right) \leq K_n, \ \forall n \geq 1 \iff \mathbf{S}_{\boldsymbol{\theta},\boldsymbol{\lambda}}(K_n) \leq \sigma_0^2 \frac{K_n}{n}, \ \forall n \geq 1.$$

By (1) of Theorem 4.1, we have

$$\mathbf{S}_{\boldsymbol{\theta},\boldsymbol{\lambda}}(K_n) \leq \sigma_0^2 \frac{K_n}{n}, \ \forall n \geq 1 \iff \mathbf{S}_{\boldsymbol{\theta},\boldsymbol{\lambda}}(k) \leq \psi(k) \text{ for all } k \in [\bar{K}].$$

Therefore, we can rewrite

$$\mathcal{F}_{\boldsymbol{K},\boldsymbol{\lambda}} = \left\{ \boldsymbol{\theta} \in \mathbb{R}^\infty : \mathbf{S}_{\boldsymbol{\theta},\boldsymbol{\lambda}}(k) \leq \psi(k) \text{ for all } k \in [\bar{K}] \right\}.$$

$\square$

Fix any n. Define $\delta = \sqrt{c\sigma_0^2/n}$ with the constant $c = \frac{1}{4} \wedge \tau$, where τ comes from Theorem 4.1. Consider assigning nonzero signals on the block $B_n = \{\pi_1, \ldots, \pi_{K_n}\}$ to construct a subset of populations.

Specifically, we define the collection of hypercubes vertices $\mathcal{V} = \{-1, 1\}^{K_n}$. For every vertex $v \in \mathcal{V}$, define a parameter vector $\boldsymbol{\theta}^{(v)} = (\theta_j^{(v)})_{j=1}^d$ as follows:

$$\theta_{\pi_i}^{(v)} = \delta \, v_i, \text{ for } i = 1, \ldots, K_n, \qquad \text{and } \theta_j^{(v)} = 0 \text{ for } j \notin B_n. \tag{32}$$

There are 2^{K_n} such vectors $\{\boldsymbol{\theta}^{(v)}\}$, and they satisfy the following property.

Lemma A.2. *For any $v \in \mathcal{V}$, the parameter vector $\boldsymbol{\theta}^{(v)}$ constructed in Equation (32) lies in $\mathcal{F}_{\boldsymbol{K},\boldsymbol{\lambda}}$.*

Proof of Theorem A.2. For any $k \in [\bar{K}]$, if $k \geq K_n$, then $\mathbf{S}_{\boldsymbol{\theta}^{(v)},\boldsymbol{\lambda}}(k)$ is 0.

If $1 \leq k \leq K_n - 1$, then $\mathbf{S}_{\boldsymbol{\theta}^{(v)},\boldsymbol{\lambda}}(k) \leq K_n \delta^2 = c\sigma_0^2 K_n/n$. Denote $k_0 = K_n - 1$ and $L = 1 + M_{k_0}$. By definition of M_{k_0}, we have $n \geq L$. Since $k \leq k_0$, we have $L \geq 1 + M_k$. We have

$$\begin{aligned} \frac{K_n}{n} &\leq \frac{K_n}{L} \\ &= \frac{k_0 + 1}{1 + M_{k_0}} \\ &\leq 2\frac{k_0}{M_{k_0}} \\ &\leq 2\frac{k}{M_k}, \end{aligned} \tag{33}$$

30

where the second last inequality is because $(1+k_0)/(1+m) \le 2k_0/m \Leftrightarrow m+k_0m \le 2k_0+2k_0m$ and the last inequality is due to (2) of Theorem 4.1. Since $2c < 1$, we see that $\sigma_0^2 c K_n/n \le \psi(k)$ for all $k < K_n$.

In either case, we have $\mathbf{S}_{\boldsymbol{\theta}^{(v)}, \boldsymbol{\lambda}}(k) \le \psi(k)$ for all $k \in [\bar{K}]$, and thus $\boldsymbol{\theta}^{(v)} \in \mathcal{F}_{\boldsymbol{K}, \boldsymbol{\lambda}}$. $\qquad\square$

For each $v \in \mathcal{V}$, let P_v be the sampling distribution of the sequence model in Equation (4) with $\boldsymbol{\theta}^* = \boldsymbol{\theta}^{(v)}$, $\sigma^2 = \sigma_0^2/n$, and $\{\xi_j\}_{j \in [d]}$ being i.i.d. from $N(0, \sigma^2)$. Let ρ be Hamming distance on $\mathcal{V}$. If v and $w \in \mathcal{V}$ differ in exactly one coordinate (i.e., $\rho(v, w) = 1$), then

- $\|\boldsymbol{\theta}^{(v)} - \boldsymbol{\theta}^{(w)}\|^2 \ge (2\delta)^2$, and

- the Kullback-Leibler divergence between P_v and P_w satisfies $\mathrm{KL}\big(P_v \,\|\, P_w\big) = \frac{1}{2\sigma^2}(2\delta)^2 = 2c \le \frac{1}{2}$, and by the Pinsker's inequality, $\|P_v \wedge P_w\| = 1 - \mathrm{TV}(P_v, P_w) \ge 1 - \sqrt{\mathrm{KL}\big(P_v \,\|\, P_w\big)/2} \ge 1/2$.

By Assouad's Lemma (Lemma 2 in Yu [49]), for any estimator $\widehat{\boldsymbol{\theta}}$ based on a sample $Y^{(n)}$ drawn from P_v, we have

$$\sup_{v \in \mathcal{V}} \mathbb{E}_v \big\| \widehat{\boldsymbol{\theta}} - \boldsymbol{\theta}^{(v)} \big\|^2 \ge K_n \frac{(2\delta)^2}{4} = c\sigma_0^2 \frac{K_n}{n}.$$

$\qquad\square$

Proof of Theorem 3.3. The upper bound is given by Theorem 3.2, so we only need to prove the lower bound. The main idea is the same as the proof for Theorem 4.3.

Let $\delta = \sqrt{c\sigma_0^2/n}$ with the constant $c = \frac{1}{4}$. Let $B_n = \{\pi_1, \ldots, \pi_{K_n}\}$. We define the collection of hypercubes vertices $\mathcal{V} = \{-1, 1\}^K$. For every vertex $v \in \mathcal{V}$, define a parameter vector $\boldsymbol{\theta}^{(v)} = (\theta_j^{(v)})_{j=1}^d$ as in Equation (32). There are 2^K such vectors $\{\boldsymbol{\theta}^{(v)}\}$. For each $v \in \mathcal{V}$, let P_v be the sampling distribution of the sequence model in Equation (4) with $\boldsymbol{\theta}^* = \boldsymbol{\theta}^{(v)}$, $\sigma^2 = \sigma_0^2/n$, and $\{\xi_j\}_{j \in [d]}$ being i.i.d. normal. Let ρ be Hamming distance on $\mathcal{V}$. The rest of the proof is identical to that of Theorem 4.3 and is omitted. $\qquad\square$

A.3   Details of Examples in Equation (9)

We provide the details of Equation (9) for illustration of the concepts of ESD and span profile through several examples.

Example A.3 (Polynomial spectrum with source condition)**.** *Assume* $\lambda_i = i^{-\beta}$ *for some* $\beta > 0$ *and the source condition* $\sum_{i=1}^d \lambda_i^{-s} \theta_i^{*2} \le R$ *with* $s > 0$*. The trade-off function satisfies*

$$\mathbf{H}_{\boldsymbol{\theta}^*, \boldsymbol{\lambda}}(k) \;=\; \frac{1}{k} \sum_{i>k} \theta_i^{*2} \;\le\; \frac{\lambda_k^s}{k} \sum_{i>k} \lambda_i^{-s} \theta_i^{*2} \;\le\; R\,k^{-(1+s\beta)},$$

which follows that $\mathbf{D}_{\boldsymbol{\theta}^*, \boldsymbol{\lambda}}(\sigma^2) \;\lesssim\; [\sigma^2]^{-\frac{1}{1+s\beta}}$. *Since* $\mathbf{D}_{\boldsymbol{\theta}^*, \boldsymbol{\lambda}}(\sigma^2) \le d$, *the optimal risk of PC estimator satisfies*

$$\mathcal{R}_*^{\mathrm{PC}} \;\lesssim\; \min\left([\sigma^2]^{\frac{s\beta}{1+s\beta}}, d\sigma^2 \right).$$

31

In Theorem A.3, we note that for $\sigma^2 = \sigma_0^2/n$, the upper bound becomes $\sigma_0^2 \min\left(n^{-\frac{s\beta}{1+s\beta}}, d/n\right)$. When $d = \infty$, this upper bound matches the well-known optimal rate under the source condition and the polynomial eigen-decay condition. When $d < \infty$, there is a phase transition around $d_0 \asymp n^{\frac{1}{1+s\beta}}$: if $d \lesssim d_0$, the upper bound is $d\sigma_0^2/n$; if $d \gtrsim d_0$, the upper bound is the same as if $d = \infty$. Using the span profile, we can extend classical results to finite-dimensional models and reveal new phenomena.

Example A.4 (Polynomial signals ($\alpha > 1$)). *Suppose $\theta_i^* = i^{-\alpha/2}$ for some constant $\alpha > 1$, and $\{\lambda_i\}_1^d$ are decreasing. By an integral approximation, we can get $\mathbf{H}_{\boldsymbol{\theta}^*,\boldsymbol{\lambda}}(k) \leq \frac{1}{\alpha-1} k^{-\alpha}$. Therefore, we have $\mathbf{D}_{\boldsymbol{\theta}^*,\boldsymbol{\lambda}}(\sigma^2) \lesssim [\sigma^2]^{-\frac{1}{\alpha}}$. The optimal risk of PC estimator satisfies*

$$\mathcal{R}_*^{\mathrm{PC}} \;\leq\; 2\sigma^2 \mathbf{D}_{\boldsymbol{\theta}^*,\boldsymbol{\lambda}}(\sigma^2) \;\lesssim\; \min\left([\sigma^2]^{1-\frac{1}{\alpha}}, d\sigma^2\right).$$

Example A.5 (Polynomial signals ($\alpha = 1$)). *Suppose $d < \infty$, $\theta_i^* = i^{-1/2}$, and $\{\lambda_i\}_1^d$ are decreasing. We show in the supplementary material that for some constant C, if $d\sigma^2 \leq e$, then $\mathcal{R}_*^{\mathrm{PC}} \leq Cd\sigma^2$, and if $d\sigma^2 > e$, then $\mathcal{R}_*^{\mathrm{PC}} \leq C\log(d\sigma^2/\log(d\sigma^2))$.*

Example A.6 (Polynomial signals ($\alpha < 1$)). *Suppose $d < \infty$, $\theta_i^* = i^{-1/2}$, and $\{\lambda_i\}$ is decreasing. We show in the supplementary material that $\mathcal{R}_*^{\mathrm{PC}} \lesssim d\min\left(d^{-\alpha}, \sigma^2\right)$.*

These examples suggest that using our framework of span profile, we are able not only to recover classical results but also to extend it to various settings where the classical framework is inapplicable.

Details of Theorem A.5. We have $\mathbf{H}_{\boldsymbol{\theta}^*,\boldsymbol{\lambda}}(k) \leq k^{-1} \int_k^d \frac{1}{x}dx = k^{-1}\left(\log d - \log k\right)$.

By dropping the term $\log k$ in the numerator, it is easy to see that a sufficient condition for $\mathbf{H}_{\boldsymbol{\theta}^*,\boldsymbol{\lambda}}(k) \leq \sigma^2$ is given by $k \geq \sigma^{-2}\log(d)$. Therefore, we have $\mathbf{D}_{\boldsymbol{\theta}^*,\boldsymbol{\lambda}}(\sigma^2) \leq \lceil\sigma^{-2}\log(d)\rceil$.

The upper bound can be improved. Suppose $A > 1$ satisfies $d\sigma^2 \leq A\log A$. If $k \geq \sigma^{-2}\log A$, then

$$\frac{k}{d} \geq \frac{\log A}{d\sigma^2} \geq \frac{d\sigma^2/A}{d\sigma^2} = \frac{1}{A},$$

which follows that $\mathbf{H}_{\boldsymbol{\theta}^*,\boldsymbol{\lambda}}(k) \leq k^{-1}\log A \leq \sigma^2$. Therefore,

$$\mathbf{D}_{\boldsymbol{\theta}^*,\boldsymbol{\lambda}}(\sigma^2) \leq \min\left(d, \lceil\sigma^{-2}\log A\rceil\right).$$

By elementary calculus, if $y > e$, the solution to $x\log x = y$ satisfies that $x \in (e, y)$, and thus $\log x \in (1, \log(y))$, which implies $x > y/\log(y)$ and thus $x < y/\log(y/\log(y)) = y/(\log y - \log\log y) < 2y/\log(y)$.

If $d\sigma^2 \leq e$, we can take $A = e$ and conclude

$$\mathcal{R}_*^{\mathrm{PC}} \;\leq\; 2\sigma^2 \mathbf{D}_{\boldsymbol{\theta}^*,\boldsymbol{\lambda}}(\sigma^2) \;\lesssim\; d\sigma^2.$$

If $d\sigma^2 > e$, then $\log(d\sigma^2) > 1$ and we can take $A = 2d\sigma^2/\log(d\sigma^2)$, which implies that

$$\mathcal{R}_*^{\mathrm{PC}} \;\leq\; 2\sigma^2 \mathbf{D}_{\boldsymbol{\theta}^*,\boldsymbol{\lambda}}(\sigma^2) \;\lesssim\; \log(d\sigma^2) - \log\left(\log(d\sigma^2)\right).$$

$\square$

Detail of Theorem A.6. By an integral approximation, we see that

$$\mathbf{H}_{\boldsymbol{\theta}^*,\boldsymbol{\lambda}}(k) \;\asymp\; k^{-1}\left(d^{1-\alpha} - k^{1-\alpha}\right).$$

32

Case 1: $\sigma^2 d^\alpha < 2$. We have the default bound $\mathbf{D}_{\boldsymbol{\theta^*},\boldsymbol{\lambda}}(\sigma^2) \leq d$.

Case 2: $\sigma^2 d^\alpha \geq 2$. If $k \geq d^{1-\alpha}/\sigma^2$, then $\mathbf{H}_{\boldsymbol{\theta^*},\boldsymbol{\lambda}}(k) \leq \sigma^2$. Therefore, we have $\mathbf{D}_{\boldsymbol{\theta^*},\boldsymbol{\lambda}}(\sigma^2) \leq \lceil d^{1-\alpha}/\sigma^2 \rceil$, which is not larger than $\lceil d/2 \rceil$.

Combining both cases, we have $\mathbf{D}_{\boldsymbol{\theta^*},\boldsymbol{\lambda}}(\sigma^2) \lesssim d\min(1/(d^\alpha\sigma^2), 1)$. Multiplying by $2\sigma^2$ on both sides, we have

$$\mathcal{R}_*^{\mathrm{PC}} \leq 2\sigma^2 \mathbf{D}_{\boldsymbol{\theta^*},\boldsymbol{\lambda}}(\sigma^2) \lesssim d\min\left(d^{-\alpha}, \sigma^2\right).$$

$\square$

A.4 Detail of Theorem 4.4

Let $f(x) = \sigma_0^2 x e^{-x^b}$. Then $(\theta_{j+1}^*)^2 = f(j) - f(j+1)$ for $j \geq 1$. Since $\theta_1^* = 0$, for any $k \geq 1$, the tail sum is

$$\sum_{j=k+1}^\infty (\theta_j^*)^2 = \sum_{j=k}^\infty (f(j) - f(j+1)) = f(k) = \sigma_0^2 k e^{-k^b},$$

since $f(N) \to 0$. As $\{\lambda_j\}$ is assumed to be decreasing, the trade-off function is $\mathbf{H}_{\boldsymbol{\theta^*},\boldsymbol{\lambda}}(k) = \frac{1}{k}\sum_{j=k+1}^\infty (\theta_j^*)^2 = \sigma_0^2 e^{-k^b}$.

For any $n \geq 3$, let $k = K_n$. By definition of the ceiling function, $k \geq (\log n)^{1/b}$, which implies $k^b \geq \log n$, and thus $e^{k^b} \geq n$. Then, $\mathbf{H}_{\boldsymbol{\theta^*},\boldsymbol{\lambda}}(k) = \sigma_0^2 e^{-k^b} \leq \sigma_0^2/n$. By Theorem 3.5, we have $\mathbf{D}_{\boldsymbol{\theta^*},\boldsymbol{\lambda}}(\sigma_0^2/n) \leq k = K_n$.

Since this holds for all sufficiently large n, we conclude that $\boldsymbol{\theta^*} \in \mathcal{F}_K$. Theorem 4.3 guarantee the optimal convergence rate is $\Theta(\sigma_0^2 K_n/n) = \Theta(\sigma_0^2(\log n)^{1/b}/n)$.

Lastly, we consider the standard source condition that for some $s > 0$, there is some constant R_s such that

$$\sum_{j=1}^\infty \lambda_j^{-s}(\theta_j^*)^2 \leq R_s. \tag{34}$$

Let's assume a polynomial eigenvalue decay $\lambda_j \asymp j^{-\gamma}$ for some $\gamma > 0$. Let S be the left hand side of Equation (34). Since $\theta_1^* = 0$, we have

$$S = \sum_{j=2}^\infty (j^{-\gamma})^{-s}(\theta_j^*)^2 = \sum_{j=2}^\infty j^{s\gamma}(\theta_j^*)^2$$

$$= \sum_{k=1}^\infty (k+1)^{s\gamma}(\theta_{k+1}^*)^2.$$

Using $(\theta_{k+1}^*)^2 = f(k) - f(k+1)$ with $f(x) = \sigma_0^2 x e^{-x^b}$:

$$S = \sum_{k=1}^\infty (k+1)^{s\gamma}(f(k) - f(k+1)).$$

Using summation by part, we have

$$S = (1+1)^{s\gamma} f(1) - \lim_{N\to\infty}(N+1)^{s\gamma} f(N+1) + \sum_{k=1}^\infty ((k+2)^{s\gamma} - (k+1)^{s\gamma})f(k+1).$$

Since $\lim_{N \to \infty} (N+1)^{s\gamma} N e^{-N^b} = 0$ for $b \geq 1$, the limit term vanishes. $f(1) = \sigma_0^2 e^{-1}$. The difference term $(k+2)^{s\gamma} - (k+1)^{s\gamma} > 0$. $f(k+1) = \sigma_0^2(k+1)e^{-(k+1)^b} > 0$. The sum $\sum_{k=1}^{\infty}((k+2)^{s\gamma} - (k+1)^{s\gamma})f(k+1)$ converges because $f(k+1)$ decays faster than any polynomial grows. Specifically, $(k+2)^{s\gamma} - (k+1)^{s\gamma} \approx s\gamma k^{s\gamma-1}$, and the sum $\sum k^{s\gamma-1}(k+1)e^{-(k+1)^b}$ converges. Therefore, S converges for any $s > 0$ and any $\gamma > 0$.

The classical theory predicts a rate of $n^{-\frac{s\gamma}{s\gamma+1}}$. Since the source condition holds for arbitrarily large s, the classical rate can be made arbitrarily close to n^{-1}. However, this n^{-1} rate ignores the logarithmic factor $(\log n)^{1/b}$ present in the true optimal rate $\Theta(\sigma_0^2(\log n)^{1/b}/n)$. Thus, the traditional convergence analysis based on the source condition is not sharp for this signal.

B   Proofs for results in Section 8

Proof of Theorem 8.3. **Upper bound**: Take $k = d^\dagger$, and we have $B(k) = k\mathbf{H}_{f^*,\lambda}(k) \leq k\sigma^2$. The variance $V(k) = \sum_{j=1}^{k}(\sigma_0^2 + \tau_j^2)/n \leq k(\sigma_0^2 + \sigma_{f,4}^2)/n = k\sigma^2$. Thus $\mathcal{R}_*^{\mathrm{PC}} \leq \mathcal{R}_k = B(k) + V(k) \leq 2k\sigma^2 = 2d^\dagger\sigma^2$.

Lower bound: Let k^* be the optimal tuning parameter. If $k^* \geq d^\dagger$, then $\mathcal{R}_* \geq d^\dagger\sigma_0^2/n$. If $k^* \leq d^\dagger - 1$, by definition of ESD, we have $\mathcal{R}_* \geq B(k^*) \geq B(d^\dagger - 1) \geq (d^\dagger - 1)\sigma^2 \geq (d^\dagger - 1)\sigma_0^2/n$. $\qquad\square$

Proof of Theorem 8.5. **Upper bound**: The upper bound follows the proof of the upper bound in Theorem 8.3. To see this, we note that since $f^* \in \mathcal{F}_{K,\boldsymbol{\lambda},n}$, we have $\|f\|_\infty^2 \leq \sigma_0^2 C_0^2$. Therefore, $\sigma^2 \leq \bar{\sigma}^2/n$. We can then apply the argument in Theorem 8.3 with σ^2 replaced by $\bar{\sigma}^2/n$.

Lower bound: We establish the lower bound using Assouad's method.

Let $m = \lfloor c_1 K \rfloor$. Consider the first m eigenfunctions $\{\psi_{\pi_j}\}_{j \leq m}$ corresponding to the largest eigenvalues $\{\lambda_{\pi_j}\}_{j \leq m}$. Define the collection of hypercubes vertices $\mathcal{V} = \{-1, 1\}^m$. For every vertex $v \in \mathcal{V}$, define a function

$$f^{(v)}(x) = \gamma \sum_{j=1}^{m} v_j \psi_{\pi_j}(x), \tag{35}$$

where the amplitude γ is to be chosen. Since $\mathbf{k}$ is (K, n)-regular, we have

$$f^{(v)}(x)^2 \leq \gamma^2 \sum_{j \leq m} \lambda_{\pi_j}^{-1} \sum_{j \leq m} \lambda_j \psi_{\pi_j}^2(x) \leq \gamma^2 C_1 n \kappa^2, \tag{36}$$

where $\kappa^2 = \sup_x \mathbf{k}(x,x) < \infty$ by assumption.

We choose

$$\gamma^2 = n^{-1} \min\left(\frac{\bar{\sigma}^2}{4(1 + C_0^2)}, \frac{\sigma_0^2 C_0^2}{C_1 \kappa^2}\right).$$

It then follows that $\|f^{(v)}\|_\infty^2 \leq \sigma_0^2 C_0^2$.

For each $v \in \mathcal{V}$, let P_v be the sampling distribution of $\{z_i = (x_i, y_i)\}_{i \leq n}$ from the regression model Equation (20) with $f^* = f^{(v)}$. Let ρ be the Hamming distance on $\mathcal{V}$. If v and $w \in \mathcal{V}$ differ in exactly one coordinate (i.e., $\rho(v, w) = 1$), then

- $\|f^{(v)} - f^{(w)}\|_{L^2(\mu)}^2 \geq (2\gamma)^2$, and

34

- the Kullback-Leibler divergence between P_v and P_w satisfies $\text{KL}\big(P_v \,\|\, P_w\big) = \frac{n}{2\sigma_0^2}(2\gamma)^2 \leq \frac{1}{2}$, where the last equation is due to the definition of the constant c. By the Pinsker's inequality, $\|P_v \wedge P_w\| = 1 - \text{TV}(P_v, P_w) \geq 1 - \sqrt{\text{KL}\big(P_v \,\|\, P_w\big)/2} = 1/2$.

By Assouad's Lemma (Lemma 2 in Yu [49]), for any estimator $\widehat{f}$ based on a sample $\{z_i = (x_i, y_i)\}_{i \leq n}$ drawn from P_v, we have

$$\sup_{v \in \mathcal{V}} \mathbb{E}_v \big\|\widehat{\boldsymbol{\theta}} - \boldsymbol{\theta}^{(v)}\big\|^2 \geq m \frac{(2\gamma)^2}{4} = c\frac{\sigma_0^2 K}{n},$$

where c is a constant that depends on C_0, κ, c_1, C_1.

$\square$

Proof of Theorem 8.6. Since

$$\mathcal{F}_{\mathbf{K},\mathbf{k}} = \bigcap_{n \geq n_0} \mathcal{F}_{K_n,\mathbf{k}}^{(n)},$$

the upper bound $\bar{\sigma}^2 K_n/n$ is immediately implied by Theorem 8.5.

The lower bound follows the same argument as in the proof of Theorem 4.3, but replace the construction of parameter vectors in Equation (32) by the construction of functions in Equation (35). Following the proof for Theorem 4.3, we use Theorem 4.1 to ensure the constructed functions all belong to $\mathcal{F}_{\mathbf{K},\mathbf{k}}$. Then the lower bound is given using Assouad's Lemma as in the proof of Theorem 8.5. Below, we provide the details for completeness.

Mercer's theorem yields

$$\mathbf{k}\left(\boldsymbol{x}, \boldsymbol{x}'\right) = \sum_{j=1}^{\infty} \lambda_j \psi_j(\boldsymbol{x}) \psi_j\left(\boldsymbol{x}'\right), \quad \boldsymbol{x}, \boldsymbol{x}' \in \mathcal{X}, \tag{37}$$

where $\{\psi_j\}_{j \geq 1}$ is a $L^2(\mathcal{X}, \mu)$-orthonormal eigenbasis. Without loss of generality, assume λ_j is sorted decreasingly.

Fix n and set $m := \lfloor c_1 K_n \rfloor$ where c_1 comes from Theorem 8.4.

For a sign vector $v = (v_j)_{j \leq m} \in \{-1, +1\}^m$, define the sequence of coefficients as

$$\theta_j^{(v)} := \begin{cases} \gamma v_j, & j \leq m, \\ 0, & j > m, \end{cases} \qquad f_v(x) := \sum_{j \geq 1} \theta_j^{(v)} \psi_j(x) = \gamma \sum_{j \leq m} v_j \psi_j(x).$$

Since $\mathbf{k}$ is (K_n, n)-regular, Equation (36) holds and reads as

$$f^{(v)}(x)^2 \leq \gamma^2 C_1 n \kappa^2.$$

If $\gamma_2 C_1 n \kappa^2 \leq \sigma_0^2 C_0^2$, then $\|f^{(v)}\|_\infty^2 \leq \sigma_0^2 C_0^2$. Furthermore, if $m\gamma^2 \leq (2n)^{-1}\sigma_0^2 K_n$, we can the same argument in Theorem A.2 (in particular, using Theorem 4.1 to dervie Equation (33)) to show that $f^{(v)} \in \mathcal{F}_{\mathbf{K},\mathbf{k}}$.

We choose

$$\gamma^2 = n^{-1} \min\left(\sigma_0^2, \frac{\bar{\sigma}^2}{4(1 + C_0^2)}, \frac{\sigma_0^2 C_0^2}{C_1 \kappa^2}\right),$$

which implies $f^{(v)} \in \mathcal{F}_{\mathbf{K},\mathbf{k}}$.

We then follows the same argument in the proof of lower bound in Theorem 8.5 to obtain

$$\sup_{v \in \mathcal{V}} \mathbb{E}_v \|\widehat{\boldsymbol{\theta}} - \boldsymbol{\theta}^{(v)}\|^2 \geq m \frac{(2\gamma)^2}{4} = c \frac{\sigma_0^2 K}{n},$$

where c is a constant that depends on C_0, κ, c_1, C_1.

$\square$

C   Proofs for Result on overparameterized gradient flow

In this section, we prove Theorem 5.2. The high-level idea is as follows: To show the ESD decreases, it is enough to show that the squared signal tail sorted by the learned eigenvalues at the new time is smaller than that at the old time. The key idea is to study how the gradient flow changes the eigenvalues depending on the signal's strength. Our analysis reveals that eigenvalues associated with the strong signal coordinates will often grow much faster than those associated with weak ones. Consequently, more of the largest learned eigenvalues correspond to the strong signals. This implies that the signal energy is concentrated in the top principal components of the learned kernel, which reduces the signal tail and thus reduces the ESD.

We first remark that for any $j \in [d]$, due to the same initialization $b_{j,k} = b_0$ for all k, one can prove that throughout the time $b_{j,k}$ (for all k) have the same value b_j. Therefore, we can rewrite the over-parameterization as $\theta_j = a_j b_j^D \beta_j$, and consider the following gradient flow

$$\begin{aligned}
\dot{a}_j &= -\nabla_{a_j} L_j = b_j^D \beta_j (z_j - \theta_j), \\
\dot{b}_j &= -\nabla_{b_j} L_j = D a_j b_j^{D-1} \beta_j (z_j - \theta_j), \\
\dot{\beta}_j &= -\nabla_{\beta_j} L_j = a_j b_j^D (z_j - \theta_j), \\
a_j(0) &= \lambda_j^{\frac{1}{2}} > 0, \quad \boldsymbol{b}(0) = b_0 > 0, \quad \boldsymbol{\beta}(0) = 0,
\end{aligned}$$
(38)

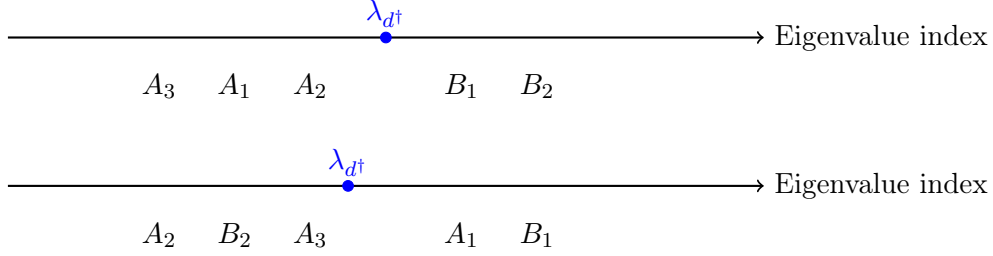where $L_j = \frac{1}{2}(z_j - \theta_j)^2$.

C.1   Proof of Theorem 5.2

Recall that we define these sets as follows:

$$\begin{aligned}
A_1 &:= \{i : \pi_{t_1}^{-1}(i) < d^\dagger(t_1), \lambda_i < c \cdot D^{-\frac{D}{D+2}} \cdot M^{\frac{2}{D+2}}, |\theta_i^*| < \tilde{\sigma}\}; \\
A_2 &:= \{i : \pi_{t_1}^{-1}(i) < d^\dagger(t_1), |\theta_i^*| > M\}; \\
A_3 &:= \{i : \pi_{t_1}^{-1}(i) < d^\dagger(t_1), |\theta_i^*| < \tilde{\sigma}\} \setminus A_1.
\end{aligned}$$

and

$$B_1 := \{i : \pi_{t_1}^{-1}(i) > d^\dagger(t_1), |\theta_i^*| < \tilde{\sigma}\}; \quad B_2 := \{i : \pi_{t_1}^{-1}(i) > d^\dagger(t_1), |\theta_i^*| > M\}.$$

where $\tilde{\sigma}^2 \leq \min\{\frac{|B_1|}{C_{B_1}}\varepsilon^2, c'\varepsilon^2\}$, $C_{B_1} = \min\{1 \vee (|A_1| - |B_1|), |B_2|\}$ and c' is a constant ≤ 1. Also recall from the assumption of Theorem 5.2 that suppose $|\theta_i^*| > |\theta_j^*| > M$, then if $C_{max}M > |\theta_i^*|$, $\eta_{i,j} = |\theta_i^*| - |\theta_j^*| > C_\eta \varepsilon'$; otherwise, $\frac{|\theta_i^*|}{|\theta_j^*|} > (1 + \frac{c_\eta}{D})$.

Throughout the proof, we assume all the events $\{E_k\}$ in Lemma C.9 hold. We divide the proof into several parts.

Part 1: Very small eigenvalues can be ignored. From Theorem 5.1, we have $\inf_{j \in S} \lambda_j > n^{-\delta}$, where δ is a constant. For $i \in R$, if $\lambda_i < n^{-(2.1\delta \vee 5)}$, Theorem C.2 implies that at t_2, we have

$$\tilde{\lambda}_i(t_2) < n^{1.1} \cdot \lambda_i^{0.99} < n^{-\delta}.$$

If B_2 is empty, then all the signals in R is 0 by the definition of $\tilde{\sigma}$. Otherwise, for $\tilde{\lambda}_i < n^{-\delta}$, and $\lambda_{\pi_{t_1}(d^\dagger(t_1))} > n^{-\delta}$. According to the monotonicity of eigenvalues in Theorem C.4, any the index i such that $\lambda_i < n^{-(2.1\delta \vee 5)}$ can not rank among the first $d^\dagger(t_1)$ at time t_2, i.e., it makes no difference to the variation of $d^\dagger$ from t_1 to t_2.

Part 2: Analysis for B_2

If $j \in B_2$, by Proposition C.1, we have $\left|\theta_j(t_2) - \theta_j^*\right| < \varepsilon' \leq \frac{1}{C_M} M$. We apply Equation (50) to get $\beta^2 = a^2 - \lambda < a^2$ and $\beta^2 = D^{-1}(b^2 - b_0^2) < D^{-1}b^2$, and thus

$$|\theta_j(t)| = a_j(t)b_j^D(t)|\beta_j(t)| \leq a_j(t)b_j^D(t) \cdot a_j^{\frac{1}{D+1}}(t) \cdot D^{-\frac{D}{2(D+1)}} b_j^{\frac{D}{D+1}}(t) = D^{-\frac{D}{2(D+1)}} \left[a_j(t)b_j^D(t)\right]^{\frac{D+2}{D+1}}.$$

Therefore, at time $t = t_2$, we have for some constants c and C that

$$D^{-\frac{D}{2(D+1)}} \left[a_j(t)b_j^D(t)\right]^{\frac{D+2}{D+1}} \geq |\theta_j(t)| \geq (1-c)M, \implies a_j(t)b_j^D(t) \geq C \cdot D^{\frac{D}{2(D+2)}} M^{\frac{D+1}{D+2}}.$$

It follows that $\tilde{\lambda}_j(t_2) \geq cD^{\frac{D}{(D+2)}} M^{\frac{2(D+1)}{D+2}}$. Moreover, for λ_j and $D^{-1}b_0^2$ that are much smaller than $c \cdot D^{-\frac{D}{D+2}} \cdot M^{\frac{2}{D+2}}$, we use Equation (50) to obtain

$$\beta_j^2 \asymp a_j^2 \asymp D^{-1}b_j^2 \asymp D^{-\frac{D}{D+2}} M^{\frac{2}{D+2}}. \tag{39}$$

Part 3: A_1 and B_2 will exchange

In the following, suppose $i \in A_1$ and $j \in B_2$. We will prove $\tilde{\lambda}_i(t_2) < \tilde{\lambda}_j(t_2)$ by contradiction. If $\tilde{\lambda}_i(t_2) \geq \tilde{\lambda}_j(t_2)$, then by Proposition C.1, we have

$$|\theta_j(t_2) - \theta_j^*| < 2\varepsilon'.$$

By Lemma C.4, we have

$$|\theta_i(t_2)| < |\theta_i^*| + \kappa_i.$$

We have $|\theta_j| > C_D|\theta_i|$ where $C_D > 1 + \frac{c}{D}$ for $M = C_M\varepsilon > C_M|\kappa_i|$. At t_2, the following holds:

$$|\beta_j(t_2)| > C_D|\beta_i(t_2)|.$$

37

It follows that $a_i^2(t_2)b_i^{2D}(t_2) > a_j^2(t_2)b_j^{2D}(t_2)$. Combined with Equation (50), we have

$$\frac{\beta_i^2(t_2) + \lambda_i}{\beta_j^2(t_2) + \lambda_j} > \left(\frac{D\beta_j^2(t_2) + b_0^2}{D\beta_i^2(t_2) + b_0^2}\right)^D > \left(\frac{C_D}{1+\delta}\right)^D = (1 + c(C_D - 1))^D. \tag{40}$$

Recall that $|\beta_i(t_2)| < \frac{1}{C_D}|\beta_j(t_2)|$ and $\beta_j^2(t_2) > CD^{-\frac{2}{D+2}}M^{\frac{2}{D+2}}$. If we choose the constant C_D such that $(1 + c(C_D - 1))^D$ is large enough, the inequality Equation (40) will implies λ_i larger than its upper bound in the definition of set A_1. (We can let $C_D = 1 + c \cdot \frac{1}{D}$.)

The contraction shows that $\tilde{\lambda}_i(t_2) < \tilde{\lambda}_j(t_2)$ for any $i \in A_1$, $j \in B_2$. If the sets A_1 and B_2 are not empty when $t = t_1$, then from t_1 to t_2, the elements of set B_2 will be arranged before those of set A_1 according to the eigenvalue index. We only need $\lambda_i < c \cdot D^{-\frac{D}{D+2}}M^{\frac{2}{D+2}}$.

For the same reason, the elements of set A_2 will be arranged before those of set A_1 at t_2.

Part 4: A_2 and B_2 will be monotonously nonincreasing

In the following, W.L.O.G we assume $\theta^*, \theta^* > 0$. We prove that given $i \in A_2$, $j \in B_2$, if $\theta_i^* > \theta_j^*$, we have $\tilde{\lambda}_i(t_2) > \tilde{\lambda}_j(t_2)$.

If $\theta_i^* - \theta_j^* > C_\eta \varepsilon$, we have $z_i > z_j$. Then by Proposition C.1, we have at t_2

$$|\theta_i(t_2) - \theta_i^*| < 2\varepsilon', \quad |\theta_j(t_2) - \theta_j^*| < 2\varepsilon'.$$

If $\lambda_i \geq \lambda_j$, by Equation (38) and monotonicity, we always have $\tilde{\lambda}_i(t) > \tilde{\lambda}_j(t)$.

Now, consider the case where $\lambda_i < \lambda_j$. By the definition of A_1 and B_2, we have $\lambda_j < c \cdot D^{-\frac{D}{D+2}} \cdot M^{\frac{2}{D+2}}$. Next, we use proof by contradiction. Note that

$$\frac{\theta_i(t_2)}{\theta_j(t_2)} = \frac{\tilde{\lambda}_i^{\frac{1}{2}}(t_2)\beta_i(t_2)}{\tilde{\lambda}_j^{\frac{1}{2}}(t_2)\beta_j(t_2)} \geq C_D.$$

If $\tilde{\lambda}_i(t) \leq \tilde{\lambda}_j(t)$, then $\beta_i(t_2) > C_D\beta_j(t_2)$. By Equation (39), both $\beta_i(t_2)$ and $\beta_j(t_2)$ are much larger then $D^{-\frac{1}{2}}b_0$. It then follows that

$$\left(\frac{D\beta_i^2(t_2) + b_0^2}{D\beta_j^2(t_2) + b_0^2}\right)^D > C^*$$

where C^* is a constant that can be made large enough by choosing C_D. Therefore, using the same reason as in Equation (40), we can get

$$\frac{\beta_i^2(t_2) + \lambda_i}{\beta_j^2(t_2) + \lambda_j} < \frac{1}{C^*},$$

which is impossible because $\beta_i(t_2) > C_D\beta_j(t_2)$ and $\beta_i^2(t_2) > C\lambda_j$.

Part 5: B_1 will stay behind A_2, A_3 and B_2

In the following, let $j \in B_1$. By $y = \theta^* + \xi$, we have $|z_j| < \tilde{\sigma} + \varepsilon'$. By Equation (53) and $|\theta_j| < |z_j|$, we have

$$|\beta_j(t_2)| \leq \left(D^{-D/2}|z_j|\right)^{1/(D+2)}.$$

Then by $\tilde{\lambda}_j(t_2) = (\beta_j^2(t_2) + \lambda_j)(D\beta_j^2(t_2) + b_0^2)^D < (1 + \frac{1}{c \cdot D})^D b_0^{2D}(\beta_j^2(t_2) + \lambda_j)$. Then if $\lambda_j < c \cdot D^{-D/(D+2)}\varepsilon^{2/(D+2)}$, given any $i \in A_3 \cup A_2 \cup B_2$, $\tilde{\lambda}_i(t_2) > \tilde{\lambda}_j(t_2)$. Otherwise, we have $\lambda_j > C \cdot D^{-D/(D+2)}\varepsilon^{2/(D+2)}$, then we have $\tilde{\lambda}_j(t_2) < (1 + \delta)\tilde{\lambda}_j(t_1)$, then by the definition of $d^\dagger$, at least $d^\dagger$ eigenvalues will larger than $\tilde{\lambda}_j(t_2)$.

Part 6: A_3 will be ahead of A_1

by the same reason between B_1 and A_1, for given $j \in A_3$, $\tilde{\lambda}_j(t_2) = (\beta_j^2(t_2) + \lambda_j)(D\beta_j^2(t_2) + b_0^2)^D < (1 + \frac{1}{c \cdot D})^D b_0^{2D}(\beta_j^2(t_2) + \lambda_j)$, and $i \in A_1$, $\lambda_i < c \cdot D^{-D/(D+2)}\varepsilon^{2/(D+2)}$, combined with

$$|\beta_i(t_2)| \leq \left(D^{-D/2}|z_i|\right)^{1/(D+2)}.$$

then we have $\tilde{\lambda}_j(t_2) > \tilde{\lambda}_i(t_2)$ for c is small and C is large enough.

Part 7: Ordering of the spectrum at t_2 and $d^\dagger(t_1) \geq d^\dagger(t_2)$

To show $d^\dagger(t_2) \leq d^\dagger(t_1)$, it suffices to show $\mathbf{H}_{\boldsymbol{\theta}^*, \tilde{\boldsymbol{\lambda}}(t_2)}(d^\dagger(t_1)) < \mathbf{H}_{\boldsymbol{\theta}^*, \tilde{\boldsymbol{\lambda}}(t_2)}(d^\dagger(t_1))$, which is equivalent to prove the following difference

$$\sum_{i:\pi_{t_1}^{-1}(i)>d^\dagger(t_1)} |\theta_i^*|^2 - \sum_{i:\pi_{t_2}^{-1}(i)>d^\dagger(t_1)} |\theta_i^*|^2 \tag{41}$$

is nonnegative.

We will make use of $|A_1| + |A_2| + |A_3| = d^\dagger(t_1)$ and consider two possible cases.

- Case 1: $|B_2| \leq |A_1|$. Since $B_2 \cup A_2$ is ahead of $A_1 \cup B_1$, we can see that the eigenvalue of the last element of $B_2 \cup A_2$ is among the top $d^\dagger$ ones. Because A_3 is ahead of $A_1 \cup B_1$, so only some of A_1 is swapped to the later part. Also some of B_1 may arise ahead some of A_1. Therefore, to analyze the ordering of eigenvalues $\tilde{\boldsymbol{\lambda}}(t_2)$, we define

$$\begin{aligned} B_{11} &= \{i \in B_1 : \pi_{t_2}^{-1}(i) \leq d^\dagger(t_1)\}. \\ A_{11} &= \{i \in A_1 : \pi_{t_2}^{-1}(i) > d^\dagger(t_1)\}. \end{aligned} \tag{42}$$

Here A_{11} contains all the elements that move from the top $d^\dagger(t_1)$ part to the later part, while B_2 and B_{11} are the elements that move from the later part to the top $d^\dagger(t_1)$ part. Therefore, we have $|A_{11}| = |B_2| + |B_{11}|$. Let $C_{B_1} := \min\{(|A_1| - |B_2|)_+, |B_1|\}$. We have $|B_{11}| \leq C_{B_1}$.

W.L.O.G., we can write divide A_{11} into two subsets such that $|A_{111}| = |B_2|$ and $|A_{112}| = |B_{11}|$. We can then write Equation (41) as

$$\|\theta_{B_2}^*\|_2^2 + \|\theta_{B_{11}}^*\|_2^2 - \|\theta_{A_{111}}^*\|_2^2 - \|\theta_{A_{112}}^*\|_2^2. \tag{43}$$

The exchange between A_1 and B_2 yields

$$\|\theta_{B_2}^*\|_2^2 - \|\theta_{A_{111}}^*\|_2^2 \geq |B_2|(M^2 - \tilde{\sigma}^2), \tag{44}$$

and

$$\|\theta_{B_{11}}^*\|_2^2 - \|\theta_{A_{112}}^*\|_2^2 \geq -|B_{11}|\tilde{\sigma}^2 \geq -C_{B_1}\tilde{\sigma}^2.$$

39

Note the assumption of Theorem 5.2 that $(|B_2| + C_{B_1})\tilde{\sigma}^2 \leq |B_2|M^2$. We add the last two inequalities Equation (43) and section C.1 together to get

$$\sum_{i:\pi_{t_1}(i)>d^\dagger(t_1)} |\theta_i^*|^2 - \sum_{i:\pi_{t_2}(i)>d^\dagger(t_1)} |\theta_i^*|^2 \geq 0,$$

where $\geq$ becomes $>$ if $B_2 \neq \emptyset$. By the definition of $d^\dagger$, $d^\dagger(t_2) \leq d^\dagger(t_1)$.

- Case 2: $|B_2| > |A_1|$. If the eigenvalue of the last element of $B_2 \cup A_2$ is among the top $d^\dagger$, we follow the exact same proof in Case 1.

  Now suppose that the eigenvalue of the last element of $B_2 \cup A_2$ is in the later part. In this case, all elements B_1 and A_1 are in the later part. We first identify all the elements that fall in the later part at time t_2: in addition to all elements of B_1, the following

$$\begin{aligned}
B_{21} &:= \{i \in B_2 : \pi_{t_2}^{-1}(i) > d^\dagger\}, \\
A_{11} &:= \{i \in A_1 : \pi_{t_2}^{-1}(i) > d^\dagger\}, \\
A_{21} &:= \{i \in A_2 : \pi_{t_2}^{-1}(i) > d^\dagger\}, \\
A_{31} &:= \{i \in A_3 : \pi_{t_2}^{-1}(i) > d^\dagger\}.
\end{aligned}$$

Note that at time t_1, the elements in the later part are in B_1, B_{21}, and $B_{22} := B_2 \setminus B_{21}$. Therefore, Equation (41) can be written as

$$\|\theta_{B_{22}}\|^2 - \|\theta_{A_{11}}\|^2 - \|\theta_{A_{21}}\|^2 - \|\theta_{A_{31}}\|^2. \tag{45}$$

By definition of B_2, A_1, and A_3, each squared element in B_2 is larger than that of both A_1 and A_3. In addition, since A_2 and B_2 will be monotonously nonincreasing, for any element in B_{22}, its squared signal will be no less than that of any element in $\theta_{A_{21}}$. Therefore, we conclude that Equation (45) is nonnegative and will be positive if B_{22} is not empty.

C.2 Generalized signal results by dynamic equation analysis

Proposition C.1 (Shrinkage monotonicity and shrinkage time). *Suppose all the events $\{E_k\}$ in Lemma C.9 hold. Let $\varepsilon = 2(C_{proxy})^{-1/2}\sqrt{\frac{\ln n\tilde{d}}{n} \cdot \ln n}, \varepsilon' = 2(C_{proxy})^{-1/2}\sqrt{\frac{\ln n}{n}}$.*
For any $j \in S$ (as defined in Theorem 5.1), we have

$$|\theta_j^* - \theta_j(t)| < 2\varepsilon'. \quad \forall t \geq t(\varepsilon) \tag{46}$$

where $t(\varepsilon) = C\, b_0^{-D}\, \varepsilon^{-1} \ln n$ for some absolute constant C.

Proof. When all the events E_k in Lemma C.9 hold, we have

$$\|\xi_S\|_\infty \leq \varepsilon'. \tag{47}$$

Consider $j \in S$. We have $\theta_j^* \geq 8\varepsilon'$ (We let $C_M \geq 8$). By taking $\delta = \varepsilon'$ and also $\kappa = \varepsilon'$ in Lemma C.7, we have

$$|\theta_j^* - \theta_j(t)| \le 2\varepsilon', \quad \forall t \ge \bar{T}^{app}(\delta),$$

with

$$\bar{T}^{app}(\delta) \le T^{\text{sig}} + C_2 D^{\frac{D}{D+2}}(\theta_j^*)^{-\frac{2D+2}{D+2}} \ln^+ \frac{2\theta_j^*}{\delta}, \tag{48}$$

and

$$T^{\text{sig}} \le \begin{cases} C_1(\theta_j^*)^{-1} b_0^{-D} \ln\left(\frac{eb_0}{a_{0j}\sqrt{D}}\right) & a_{0j} < b_0/\sqrt{D}; \\ C_1(\theta_j^*)^{-1} a_{0j}^{-1} \ln\left(\frac{ea_{0j}\sqrt{D}}{b_0}\right) & a_{0j} > b_0/\sqrt{D}, \text{ and } D = 1; \\ C_1(\theta_j^*)^{-1} D^{-\frac{1}{2}} a_{0j}^{-1} b_0^{-D+1} & a_{0j} > b_0/\sqrt{D}, \text{ and } D > 1, \end{cases} \tag{49}$$

where both C_1 and C_2 are absolute constants.

For the choice $b_0 = cD^{\frac{D+1}{D+2}}\varepsilon^{\frac{1}{D+2}}$, the second term on the right-hand side of Equation (48) is dominated by the right-hand side of Equation (49), and we can choose c small enough so that the summation of the two terms is bounded by $b_0^{-D}\varepsilon^{-1}\ln n$. This justifies our choice of $t(\varepsilon)$.

$\square$

Proposition C.2. *We consider the set R. We let $j \in R$, and suppose all the events $\{E_k\}$ in Lemma C.9 hold. Given b_0 and $t(\varepsilon)$ defined in Proposition C.1. For any positive constant δ', if the eigenvalue $\lambda_j < n^{-5}$, and n is large enough, then we have*

$$\tilde{\lambda}_j(t) < 2\lambda_j^{1-2\delta'} b_0^D \cdot n^{1+\delta'}.$$

Proof. Since the events in Lemma C.9 hold, we have $|\xi_j| \le 2(C_{\text{proxy}})^{-1/2}\sqrt{\frac{\ln\tilde{j}+\ln n}{n}}$, where $\tilde{j} = \frac{\tilde{d}}{\lambda_j}$. Since $j \in R$, we have $|\theta_j^*| \le \tilde{\sigma} \le \sqrt{c'}\varepsilon$. Since $b_0^D t(\varepsilon) = \varepsilon^{-1}\ln n$, we can check that t is no more than the hitting time T_2 defined by Equation (67) in Theorem C.8 as follows.

Note that

$$\varepsilon^{-1}\ln n(|\theta_j^*| + |\xi_j|) \le \sqrt{c'}\ln n + \sqrt{\ln n}\sqrt{\frac{n}{\ln n\tilde{d}}} \cdot \sqrt{\frac{\ln n\tilde{d} + \ln\frac{1}{\lambda_j}}{n}}$$

$$< \ln n + \sqrt{\ln n + \ln\frac{1}{\lambda_j}}.$$

Since $b_0 = c \cdot D^{\frac{D+1}{D+2}}\varepsilon^{\frac{1}{D+2}}$, for n large enough, we have $\lambda_j < n^{-5} < \frac{b_0^2}{D^2}$ and also

$$\ln\frac{b_0/D}{\lambda_j^{\frac{1}{2}}} = \ln c + \frac{1}{2(D+2)}(\ln n + \ln\ln n\tilde{d}) - \frac{1}{D+2}\ln D + \frac{1}{2}\ln\frac{1}{\lambda_j} > \ln n + \sqrt{\ln n + \ln\frac{1}{\lambda_j}}.$$

It then follows that

$$\beta_j(t) < \lambda_j^{\frac{1}{2}} \exp\left(b_0^D t(|\theta_j^*| + |\xi_j|)\right)$$

$$\leq \lambda_j^{\frac{1}{2}} \exp\left(\sqrt{\ln n}\sqrt{\frac{n}{\ln n\tilde{d}}} \cdot \sqrt{\frac{\ln n\tilde{d} + \ln\frac{1}{\lambda_j}}{n}}\right) \cdot n$$

$$< \lambda_j^{\frac{1}{2}} \exp\left(\sqrt{\ln\frac{1}{\lambda_j}}\right) \cdot \exp\left(\sqrt{\ln n}\right) \cdot n$$

$$< \lambda_j^{\frac{1}{2} - \delta'} n^{1 + \delta'}.$$

Using $\tilde{\lambda}_j(t) = (\beta_j^2(t) + \lambda_j)(b_0^2 + D\beta_j^2(t))^D$, we obtain the desired result for sufficiently large n. $\qquad\square$

Remark C.3. *The above proposition provides a very weak upper bound on $\tilde{\lambda}$, but it is sufficient to show that any eigenvalue λ_j, such that if given any constant C, $\lambda_j < n^{-C}$, then $\tilde{\lambda}_j(t)$ is also less than any polynomial of n^{-1}. Therefore, when considering the eigenvalue ordering problem, such signals can be ignored.*

C.3   Conservation quantity

We omit the subscript j in the following two sections C.3 and C.4 because all the proofs are similar for $j = 1, 2, \cdots, d$. By Equation (38), it is easy to see that

$$\frac{d}{dt}a^2 = \frac{1}{D}\frac{d}{dt}b^2 = \frac{d}{dt}\beta^2 = 2ab^D\beta(\theta^* - \theta + \xi).$$

Consequently, we have

$$a^2(t) - \beta^2(t) \equiv a_0^2, \quad b^2(t) - D\beta^2(t) \equiv b_0^2. \tag{50}$$

Using this, we see that

$$a(t) = \left(\beta^2(t) + a_0^2\right)^{1/2}, \qquad b(t) = \left(D\beta^2(t) + b_0^2\right)^{1/2} > 0.$$

Using these conservation quantities, we can prove the following estimations in terms of β:

$$\max\left(a_0, |\beta|\right) \leq a \leq \sqrt{2}\max\left(a_0, |\beta|\right)$$
$$\max\left(b_0, \sqrt{D}|\beta|\right) \leq b \leq \sqrt{2}\max\left(b_0, \sqrt{D}|\beta|\right) \tag{51}$$

which also implies that $|\theta| = \left|ab^D\beta\right| \geq D^{D/2}|\beta|^{D+2}$. The evolution of θ. It is direct to compute that

$$\dot{\theta} = \dot{a}b^D\beta + aDb^{D-1}\dot{b}\beta + ab^D\dot{\beta}$$
$$= \left[\left(b^D\beta\right)^2 + \left(Dab^{D-1}\beta\right)^2 + \left(ab^D\right)^2\right](\theta^* - \theta + \xi) \tag{52}$$
$$= \theta^2\left(a^{-2} + D^2b^{-2} + \beta^{-2}\right)(\theta^* - \theta + \xi).$$

And we also have

$$|\theta| = \left|ab^D\beta\right| \geq D^{D/2}|\beta|^{D+2} \quad \Longrightarrow \quad |\beta| \leq \left(D^{-D/2}|\theta|\right)^{1/(D+2)}. \tag{53}$$

Therefore,

$$\theta^2\left(a^{-2} + D^2b^{-2} + \beta^{-2}\right) \geq \theta^2\beta^{-2} \geq D^{-\frac{D}{D+2}}|\theta|^{\frac{2D+2}{D+2}}. \tag{54}$$

C.4 Multi-layer dynamic

We study the dynamic of the ODE for any given j. Before the analysis, we streamline some notations.

Assume for some $\kappa_j > 0$, it holds that $|\xi_j| \leq \kappa_j$. (Note that this κ_j can be the high probability upper bound derived using Theorem C.9.) Since j is given, we drop the the subscript j to simplify the exposition throughout this subsection; for example, we write λ for λ_j and θ^* for θ_j^*. We write $\ln^+(x) = \max(1, \ln(x))$ for any $x > 0$.

Lemma C.4 (Monotonicity from equation). *Consider the equation Equation (38). Suppose $y > 0$.*

1. *$a(t), \beta(t),$ and $\theta(t)$ are all non-negative and increasing.*

2. *We have*
$$y \geq \theta(t) \geq 0 \quad \forall t \geq 0.$$

3. *Since $y = \theta^* + \xi$ and $|\xi| \leq \kappa$, we have*
$$|\theta^* - \theta(t)| \leq |\theta^*| + \kappa, \quad \forall t \geq 0.$$

4. *$|\theta^* - \theta(t)|$ is decreasing provided that $|\theta^* - \theta(t)| > \kappa$.*

5. *If $|\theta^* - \theta(t_1)| \leq \kappa$ for some t_1, we have*
$$|\theta^* - \theta(t)| \leq \kappa \text{ for all } t \geq t_1.$$

If $y < 0$, Items 3, 4, and 5 still hold, while Items 1 and 2 can be modified by symmetry.

Proof. Items 1 and 2 are directly implied from Equation (38). Item 3 is implied by Item 2.

To prove Item 4, consider Equation (52), from which we have

$$\dot{\theta} = \theta^2\left(a^{-2} + D^2b^{-2} + \beta^{-2}\right)(y - \theta),$$

which implies $\dot{\theta} \geq 0$.

Since $|\theta^* - \theta(t)| > \kappa$, we have either $\theta(t) > \theta^* + \kappa$ or $\theta(t) < \theta^* - \kappa$.

The first case is not possible; otherwise, we have $0 < y = \xi + \theta^* \leq \kappa + \theta^* < \theta \leq y$, which is a contradiction. In the second case, we have $|\theta^* - \theta(t)| = \theta^* - \theta(t)$, which is decreasing because $\dot{\theta} \geq 0$.

Item 5 is implied by Item 4.

$\square$

Lemma C.5 (Approaching from below). *Consider the equation Equation (38). Suppose $\theta^* \geq 8\kappa$ (similar results hold for $\theta^* \leq -8\kappa$ by symmetry). Suppose $t_0 \geq 0$ such that $0 \leq \theta(t_0) < \frac{1}{4}\theta^*$. Define*

$$T^{sig} = \inf\left\{s \geq 0 : \theta(t_0 + s) \geq \theta^*/4\right\}.$$

This is the extra time needed from t_0 for θ to reach $\theta^*/4$. We have

$$T^{sig} \leq \begin{cases} 4(\theta^*)^{-1}b_0^{-D}\ln\left(\frac{b_0}{a_0\sqrt{D}}\right) & a_0 < b_0/\sqrt{D}; \\ 4(\theta^*)^{-1}a_0^{-1}\ln\left(\frac{a_0\sqrt{D}}{b_0}\right) & a_0 > b_0/\sqrt{D}, \quad and \quad D = 1; \\ 4(\theta^*)^{-1}D^{-\frac{1}{2}}a_0^{-1}b_0^{-D+1} & a_0 > b_0/\sqrt{D}, \quad and \quad D > 1. \end{cases} \tag{55}$$

Proof. Since $|y - \theta^*| = |\xi| \leq \kappa$ and $\theta^* \geq 8\kappa$, we have $y \geq 7\kappa > 0$. Therefore, $\theta(t) \in [0, y]$. For any $t \leq t_0 + T^{\text{sig}}$, we use $\theta^* \geq 8\kappa$ to show that

$$y - \theta(t) = \theta^* - \theta(t) + \xi \geq \frac{3}{4}\theta^* - \kappa \geq \frac{1}{2}\theta^*.$$

Let $r = \min\left(a_0, b_0/D^{\frac{1}{2}}\right)$ and $R = \max\left(a_0, b_0/D^{\frac{1}{2}}\right)$. Define the following time point if it exists:

$$T^{\text{pos},1} = \inf\left\{s \geq 0 : \beta(t_0 + s) \geq r\right\}; \quad T^{\text{pos},2} = \inf\left\{s \geq 0 : \beta(t_0 + s) \geq R\right\}$$

$$T^{\text{sig}} = \inf\left\{s \geq 0 : |\theta^* - \theta(t_0 + s)| \leq \frac{3}{4}\theta^*\right\}.$$

We will first bound both $T^{\text{pos},1}$ and $T^{\text{pos},2}$.

From Equation (38), we have

$$\dot{\beta}(t) = a(t)b^D(t)[\theta^* + \xi - \theta(t)] \geq \frac{1}{4}\theta^* a(t)b^D(t), \quad \text{for} \quad t \leq t_0 + T^{\text{sig}}. \tag{56}$$

Stage 1: $0 \leq s \leq T^{\text{pos},1}$. Note that $\sqrt{2}a_0 > a(t) > a_0$, and $e \cdot b_0^D > b(t)^D = (D\beta(t)^2 + b_0^2)^{\frac{D}{2}} > b_0^D$. We have

$$\dot{\beta}(t_0 + s) \geq \frac{1}{4}\theta^* a_0 b_0^D \geq \frac{1}{4}\theta^* a_0 b_0^D,$$

which suggests β increases at least linearly. Therefore, we have

$$T^{\text{pos},1} \leq 8r\left(\theta^* a_0 b_0^D\right)^{-1}. \tag{57}$$

Stage 2: $T^{\text{pos},1} \leq s \leq T^{\text{pos},2}$. Consider two cases.

Case 1: If $a_0 < b_0/\sqrt{D}$, $r = a_0$ and $R = b_0/\sqrt{D}$. Note $a \geq \beta$ in Equation (51). We use Equation (56) to get

$$\dot{\beta}(t_0 + s) \geq \frac{1}{4}\theta^* b_0^D |\beta(t_0 + s)|,$$

By Grönwall's inequality, we have

$$T^{\text{pos},2} - T^{\text{pos},1} \leq 4\left(\theta^* b_0^D\right)^{-1}\ln\frac{b_0}{a_0\sqrt{D}}. \tag{58}$$

44

Case 2: If $a_0 > b_0/\sqrt{D}$, $R = a_0$ and $r = b_0/\sqrt{D}$. We use $b \geq \sqrt{D}\beta$ in Equation (51) together with $a > a_0$, $b > \sqrt{D}|\beta|$ and Equation (56) to get that

$$\dot{\beta}(t_0 + s) \geq \frac{1}{4}\theta^* a_0 D^{\frac{D}{2}} |\beta(t_0 + s)|^D.$$

By comparison theorem, we have

$$T^{\text{pos},2} - T^{\text{pos},1} \leq \begin{cases} 4(\theta^* a_0)^{-1} \ln \frac{a_0 \sqrt{D}}{b_0}, & \text{if} \quad D = 1; \\ 4\left((D-1)\theta^* a_0 D^{D/2}\right)^{-1} \left[\left(b_0/\sqrt{D}\right)^{-(D-1)} - a_0^{-(D-1)}\right], & \text{if} \quad D \geq 2. \end{cases}$$
(59)

Stage 3: If $T^{\text{sig}} \leq T^{\text{pos},2}$, then we can use the for T^{sig} in Stage 2 as a bound for T^{sig}. Now, we consider the case $T^{\text{pos},2} < T^{\text{sig}}$. We combine Equation (51) with $a > |\beta|$, $b > \sqrt{D}|\beta|$, and Equation (56) to get

$$\dot{\beta}\left(t_0 + T^{\text{pos},2} + s\right) \geq \frac{1}{4}\theta^* D^{D/2}|\beta\left(T^{\text{pos},2} + s\right)|^{D+1}, \quad \text{for} \quad s \in \left[0, T^{\text{sig}} - T^{\text{pos},2}\right].$$

Beside, we have $\beta\left(t_0 + T^{\text{pos},2}\right) = R > 0$. By Lemma C.10, we have

$$T^{\text{sig}} - T^{\text{pos},2} \leq 4D^{-\frac{D+2}{2}}(\theta^*)^{-1}R^{-D}.$$
(60)

We now bound T^{sig} using the summation of Equation (57), Equation (60), and Equation (58) if $a_0 < b_0/\sqrt{D}$, or the summation of Equation (57), Equation (60), and Equation (59) if $a_0 > b_0/\sqrt{D}$.

If $a_0 < b_0/\sqrt{D}$, we can bound the right hand sides of Equation (57) and Equation (60) by $8(\theta^*)^{-1}b_0^{-D}$ and $4(\theta^*)^{-1}b_0^{-D}$ respectively.

If $a_0 > b_0/\sqrt{D}$, we can bound the right hand sides of Equation (57) and Equation (60) by $8(\theta^*)^{-1}D^{-\frac{1}{2}}a_0^{-1}b_0^{-D+1}$ and $4(\theta^*)^{-1}D^{-\frac{1}{2}}a_0^{-1}b_0^{-D+1}$ respectively. Furthermore, if $D > 1$, we can bound Equation (59) by $4(\theta^*)^{-1}(D-1)^{-1}D^{-\frac{1}{2}}a_0^{-1}b_0^{-D+1}$.

This leads to

$$T^{\text{sig}} \leq \begin{cases} 4(\theta^*)^{-1}b_0^{-D}\left(3 + \ln\left(\frac{b_0}{a_0\sqrt{D}}\right)\right) & a_0 < b_0/\sqrt{D}; \\ 4(\theta^*)^{-1}a_0^{-1}\left(3 + \ln\left(\frac{a_0\sqrt{D}}{b_0}\right)\right) & a_0 > b_0/\sqrt{D}, \quad \text{and} \quad D = 1; \\ 16(\theta^*)^{-1}D^{-\frac{1}{2}}a_0^{-1}b_0^{-D+1} & a_0 > b_0/\sqrt{D}, \quad \text{and} \quad D > 1. \end{cases}$$
(61)

$\square$

Lemma C.6 (Approximation time near θ^*). *Consider the equation Equation (38) with $\theta^* \geq 0$ (a similar result holds for $\theta^* \leq 0$). Suppose $\theta^* > 8\kappa$. Suppose for some $t_0 \geq 0$ such that*

$$\frac{1}{4}\theta^* \leq \theta(t_0) \leq \theta^* - \kappa.$$

Then, for any $\delta > 0$, we have

$$|\theta^* - \theta(t)| \leq \kappa + \delta, \quad \forall t \geq t_0 + 4^{\frac{2D+2}{D+2}} D^{\frac{D}{D+2}}(\theta^*)^{-\frac{2D+2}{D+2}} \ln^+ \frac{|\theta^* - \theta(t_0)| - \kappa}{\delta}.$$

Proof. Given any $\delta > 0$, if $\theta(t_0) \geq \theta^* - \kappa - \delta$, we have $|\theta^* - \theta(t)| \leq \kappa + \delta$ for all $t \geq t_0$ by Theorem C.4 (Item 4) and the desired result is proved.

Next, suppose $\theta(t_0) < \theta^* - \kappa - \delta$. Define

$$T^{\mathrm{app}} = \inf \left\{ s \geq 0 : |\theta^* - \theta(t_0 + s)| \leq \kappa + \delta \right\}.$$

By Theorem C.4 (Item 4) again, it suffices to provide an upper bound on T^{app}.

For all $t \geq t_0$, we have $\frac{1}{4}\theta^* \leq \theta(t)$ by Theorem C.4 (Item 1). Consequently, Equation (54) implies that

$$\theta^2 \left(a^{-2} + D^2 b^{-2} + \beta^{-2} \right) \geq D^{-\frac{D}{D+2}} |\theta|^{\frac{2D+2}{D+2}} \geq 4^{-\frac{2D+2}{D+2}} D^{-\frac{D}{D+2}} (\theta^*)^{\frac{2D+2}{D+2}} := c_0.$$

Furthermore, by Equation (52), we have

$$\dot{\theta} = \theta^2 \left(a^{-2} + D^2 b^{-2} + \beta^{-2} \right) (\theta^* - \theta + \xi) \geq c_0 (\theta^* - \kappa - \theta).$$

Let $x(s) := \theta^* - \kappa - \theta(t_0 + s)$ with $x(0) = \theta^* - \kappa - \theta(t_0)$. Note that T^{app} is the hitting time of $x(s)$ to δ. Applying Theorem C.11 to $x(s)$, we have

$$T^{\mathrm{app}} \leq c_0^{-1} \ln \frac{|\theta^* - \theta(t_0)| - \kappa}{\delta}.$$

$\square$

Lemma C.7. *Consider the equation Equation (38) with $\theta^* \geq 0$ (a similar result holds for $\theta^* \leq 0$).*

Suppose $\theta^* \geq 8\kappa$. For two absolute constants C_1, C_2, we have

$$|\theta^* - \theta(t)| \leq \kappa + \delta, \quad \forall t \geq \bar{T}^{app}(\delta),$$

where

$$\bar{T}^{app}(\delta) := \bar{T}^{sig} + C_2 D^{\frac{D}{D+2}} (\theta^*)^{-\frac{2D+2}{D+2}} \ln^+ \frac{\theta^*}{\delta}, \tag{62}$$

and

$$\bar{T}^{sig} := \begin{cases} C_1 (\theta^*)^{-1} b_0^{-D} \ln \left(\frac{b_0}{a_0 \sqrt{D}} \right) & a_0 < b_0 / \sqrt{D}; \\ C_1 (\theta^*)^{-1} a_0^{-1} \ln \left(\frac{a_0 \sqrt{D}}{b_0} \right) & a_0 > b_0 / \sqrt{D}, \quad and \quad D = 1; \\ C_1 (\theta^*)^{-1} D^{-\frac{1}{2}} a_0^{-1} b_0^{-D+1} & a_0 > b_0 / \sqrt{D}, \quad and \quad D > 1. \end{cases} \tag{63}$$

Proof. We will repeatedly apply the monotonicity of Theorem C.4.

Recall T^{sig} defined in Theorem C.5 with $t_0 = 0$ and let t_1 be the upper bound on T^{sig} we found therein. Then $\theta(t_1) \geq \frac{\theta^*}{4}$.

We then apply Theorem C.6 with $t_0 = t_1$, and conclude that $|\theta^* - \theta(t)| \leq \kappa + \delta$ for all $t \geq t_1 + t_2$, where $t_2 = 4^{\frac{2D+2}{D+2}} D^{\frac{D}{D+2}} (\theta^*)^{-\frac{2D+2}{D+2}} \ln^+ \frac{|\theta^* - \theta(t_1)| - \kappa}{\delta}$. Note that $|\theta^* - \theta(t_1)| - \kappa \leq \theta^*$. We complete the proof by defining $\bar{T}^{\mathrm{sig}} = t_1$ and $\bar{T}^{app}(\delta) = t_1 + 4^{\frac{2D+2}{D+2}} D^{\frac{D}{D+2}} (\theta^*)^{-\frac{2D+2}{D+2}} \ln^+ \frac{\theta^*}{\delta}$.

$\square$

Lemma C.8. *Consider the equation Equation* (38). *Denote* $r' = \min\{a_0, b_0/D\}, R' = \max\{a_0, b_0/D\}$. *W.L.O.G., We assume that* $\theta^* \geq 0$. *Define* $T_1 = \inf\{t : |\beta(t)| > r'\}$, *and* $T_2 = \inf\{t : |\beta(t)| > R'\}$. *If* $D \geq 1$, *and* t *satisfies the following:*

$$\sqrt{2}ea_0b_0^D \int_0^t (|\theta^*| + |\xi|)\mathrm{d}s \leq \min(a_0, b_0/D),$$

then we have

$$|\theta(t)| \leq 2e \cdot a_0^2 b_0^{2D} \int_0^t (|\theta^*| + |\xi|)\mathrm{d}s. \tag{64}$$

Moreover, if $a_0 \leq b_0/D$ *and* $0 \leq t \leq T_2 - T_1$ *satisfies the following:*

$$\sqrt{2}eb_0^D \int_0^t (|\theta^*| + |\xi|)\mathrm{d}s \leq \ln \frac{b_0/D}{a_0},$$

then we have

$$|\beta(t)| \leq a_0 \exp\left(b_0^D \int_0^t (|\theta^*| + |\xi|)\mathrm{d}s \right);$$

$$|\theta(t)| \leq \sqrt{2}ea_0^2 b_0^D \exp\left(2\sqrt{e}b_0^D \int_0^t (|\theta^*| + |\xi|)\mathrm{d}s \right).$$

Proof. From Equation (38), we have

$$|\beta(t)| \leq \int_0^t a(s)b^D(s)(|\theta^*| + |\xi|)\mathrm{d}s.$$

Consider $t \leq T_1$. We use Equation (51) to get $a(t) \leq \sqrt{2}a_0$ and by Equation (50), $b^2(t) - D\beta^2(t) \equiv b_0^2$. Consequently, we have $b^2(t) \leq (1 + \frac{1}{D})b_0^2$, and thus

$$|\beta(t)| \leq \sqrt{2}ea_0b_0^D \int_0^t (|\theta^*| + |\xi|)\mathrm{d}t, \tag{65}$$

which implies Equation (64) by using the fact that $|\theta| = |ab^D\beta|$. Furthermore, Equation (65) implies that

$$T_1 \geq \inf\left\{ t \geq 0 : \sqrt{2}ea_0b_0^D \int_0^t (|\theta^*| + |\xi|)\mathrm{d}s \geq r' \right\}.$$

Then when $t > T_1$, in the following, suppose $a_0 \leq b_0/D$. We have $r' = a_0$ and $R' = b_0/D$.

Consider $t \in (T_1, T_2)$. We have $a(t) \leq \sqrt{2}|\beta(t)|$ and $b(t)^2 \leq (1 + \frac{1}{D})b_0^2$. Consequently, Equation (38) implies that

$$|\beta(t)| \leq a_0 + \sqrt{2}eb_0^D \int_{T_1}^t |\beta(s)|(|\theta^*| + |\xi|)\mathrm{d}s, \tag{66}$$

for any $t \in (T_1, T_2)$. By Grönwall inequality, we have

$$|\beta(t)| \leq a_0 \exp\left(\sqrt{2}eb_0^D \int_{T_1}^t (|\theta^*| + |\xi|)\mathrm{d}s \right), \quad t \in (T_1, T_2).$$

47

By definition of T_2, we have

$$T_2 \geq \inf \left\{ t \geq T_1 : \sqrt{2e} b_0^D \int_{T_1}^t (|\theta^*| + |\xi|) \mathrm{d}s = \ln \frac{b_0/D}{a_0} \right\}. \tag{67}$$

The bound for $\theta(t)$ now follows from using the bounds $a(t) \leq \sqrt{2}|\beta|, b^2(t) \leq (1 + \frac{1}{D}) b_0^2$ to get

$$|\theta(t)| = |ab^D \beta| \leq \sqrt{2e} b_0^D |\beta|^2 \leq \sqrt{2e} a_0^2 b_0^D \exp \left(2\sqrt{e} b_0^D \int_{T_1}^t (|\theta^*| + |\xi|) \mathrm{d}s \right), \forall t \in (T_1, T_2).$$

$\square$

C.5 Auxiliary Lemma

The following lemma provides a choice of $\kappa_j \geq |\xi_j|$ with high probability.

Lemma C.9. *Recall S defined by Assumption 5.1 and let $C = 2(C_{proxy})^{-1/2}$. For $k \in S$, we introduce the events $\{E_k\}$ as follows:*

$$E_k := \{|\xi_k| \leq C n^{-1/2} \sqrt{\ln n}\}. \tag{68}$$

For $k \in S^C$, we introduce the events $\{E_k\}$ as follows:

$$E_k := \left\{ |\xi_k| \leq C n^{-1/2} \sqrt{\ln \left(n\tilde{k} \right)} \right\}. \tag{69}$$

where $\tilde{k} = \sum_j \lambda_j / \lambda_k$.

Then, with probability at least $1 - \frac{4}{n}$, all events $E_k, k \in [d]$ hold simultaneously.

Proof. By Theorem 5.1, the noise ξ_k is sub-Gaussian with variance proxy C_{proxy}/n. Therefore, $\mathbf{P}(|\xi_k| \geq s) \leq 2\exp(-(2C_{\text{proxy}})^{-1} n s^2)$.

If $k \in S$, we have

$$\mathbf{P} \left\{ |\xi_k| \geq 2 C_{\text{proxy}}^{-1/2} \sqrt{\frac{\ln n}{n}} \right\} \leq 2\exp\left(-2(\ln n)\right).$$

By the union bound, we have

$$\begin{aligned}
\mathbf{P} \{\cap_{k \in S} E_k\} &\geq 1 - \sum_{k \in S} \mathbf{P} \left\{ |\xi_k| \geq 2 C_{\text{proxy}}^{-1/2} \sqrt{\frac{\ln n}{n}} \right\} \\
&\geq 1 - |S| 2\exp\left(-2(\ln n)\right) \\
&\geq 1 - \frac{2}{n},
\end{aligned} \tag{70}$$

where the last inequality is because $|S| 2\exp\left(-2(\ln n)\right) \leq 2n^{-1}$.

48

If $k \in S^C$, we have

$$\mathbf{P}\left\{|\xi_k| \geq 2(C_{\text{proxy}})^{-1/2}\sqrt{\frac{\ln n\tilde{k}}{n}}\right\} \leq 2\exp\left(-(\ln n + \ln\frac{\sum_j \lambda_j}{\lambda_k})\right) \leq \frac{2}{n} \cdot \frac{\lambda_k}{\sum_j \lambda_j}, \quad (71)$$

where we recall that $\tilde{k} = \frac{\sum_j \lambda_j}{\lambda_k}$.

By the union bound, we have

$$\begin{aligned}
\mathbf{P}\left\{\cap_{k \in S^C} E_k\right\} &\geq 1 - \sum_{k \in S^C} \mathbf{P}\left\{|\xi_k| \geq 2(C_{\text{proxy}})^{-1/2}\sqrt{\frac{\ln n\tilde{k}}{n}}\right\} \\
&\geq 1 - \sum_{k \in S^C} \frac{2}{n} \cdot \frac{\lambda_k}{\sum_j \lambda_j} \\
&\geq 1 - \frac{2}{n}.
\end{aligned} \quad (72)$$

We combined the Equation (70) and Equation (72), and we derive the results.

$\square$

The following two lemmas provide convenient upper bounds on hitting times of ODE solutions.

Lemma C.10. *Let $k > 0$ and $p > 1$.*

- *Consider the ODE*

$$\dot{x} \geq kx^p, \quad x(0) = x_0 > 0$$

Then we have

$$x(t) \geq \left(x_0^{-(p-1)} - (p-1)kt\right)^{-\frac{1}{p-1}}$$

and thus for any $M \geq 0$,

$$\inf\{t \geq 0 : x(t) \geq M\} \leq \left[(p-1)kx_0^{p-1}\right]^{-1}. \quad (73)$$

- *Consider the ODE*

$$\dot{x} \leq -kx^p, \quad x(0) = x_0 > 0.$$

Then we have

$$x(t) \leq \left(x_0^{-(p-1)} + (p-1)kt\right)^{-\frac{1}{p-1}},$$

and thus for any $M > 0$,

$$\inf\{t \geq 0 : x(t) \leq M\} \leq \left[(p-1)kM^{p-1}\right]^{-1}. \quad (74)$$

Lemma C.11. *Let $k > 0$ and $x_0 > 0$.*

1. If

$$\dot{x}(t) \;\geq\; k\,x(t), \qquad x(0) = x_0,$$

then for all $t \geq 0$, it holds that

$$x(t) \;\geq\; x_0\,e^{kt},$$

and for every $M \geq x_0$, we have

$$\inf\{t \geq 0 : x(t) \geq M\} \;\leq\; \frac{1}{k}\log\!\left(\frac{M}{x_0}\right).$$

2. If

$$\dot{x}(t) \;\leq\; -k\,x(t), \qquad x(0) = x_0,$$

then for all $t \geq 0$, it holds that

$$x(t) \;\leq\; x_0\,e^{-kt},$$

and for every $0 < M \leq x_0$, we have

$$\inf\{t \geq 0 : x(t) \leq M\} \;\leq\; \frac{1}{k}\log\!\left(\frac{x_0}{M}\right).$$

D Related works on principal component regression

As discussed in Section 3.1, the PC estimator serves as a motivating example for the concepts of ESD and span profile due to its clear illustration of bias-variance trade-offs. However, the ESD and span profile are designed to characterize the intrinsic difficulty of generalization arising from signal-kernel alignment, and their definition do not rely on the PC estimator. Nonetheless, the analysis of PC estimators, particularly in high-dimensional linear regression, been an active area of recent research. Below, we briefly summarize some relevant contributions to provide context.

D.1 Proportional Asymptotic Limits

Several studies analyze Principal Component Regression (PCR) in the proportional asymptotic setting where the dimension p and sample size n grow with $p/n \to \gamma$. In this regime, Xu and Hsu [46] studied the limiting risk of PCR with Gaussian designs with diagonal covariance. They assume polynomially decaying eigenvalues or convergent empirical spectra and an isotropic prior and reveal a "double-descent" risk curve. In a related vein, Wu and Xu [45] extend the analysis to general covariance Σ_x and an anisotropic prior satisfying $\mathbb{E}\beta_*\beta_*^\top = \Sigma_\beta$. They also

derive an exact risk expression and demonstrate how "misalignment" between Σ_x and Σ_β affects risk; here "alignment" refers to concordance between the orderings of their eigenvalues. Both studies assume knowledge of the eigenvectors of the population covariance matrix Σ_x to construct the *oracle PCR*. Gedon et al. [17] analyze the limiting risk of PCR under a latent factor model and explore the effect of distribution shift. Green and Romanov [20] derive the exact limits of estimation risk, in-sample prediction risk, and out-of-sample prediction risk of PCR under the assumption that both the empirical distribution of the spectrum and the distribution of mass of the true signal over the eigenspace of Σ_x converges weakly.

D.2   Non-Asymptotic Analysis

Complementary research develops non-asymptotic guarantees. Agarwal et al. [1] derive finite-sample upper bounds on prediction error using $\|\beta^*\|_1^2$ and the rank of design matrix under latent factor models and explore the robustness of PCR to noise and missing values in the observed covariates. Bing et al. [9] consider PCR with adaptively selected number of components under latent factor models and provide alternative finite-sample risk bounds using $\|\beta^*\|_2^2$. Huang et al. [21] derived non-asymptotic risk bounds for PCR in more general settings by analyzing the alignment between population and empirical principal components. Hucker and Wahl [22] derive non-asymptotic error bounds for PCR in kernel regression.